Identifying emission sources for EMC improvements

Analyzing the origin and propagation of electromagnetic emissions from an electronic device

Ida Gustafsson

April 2024

Master's Thesis in
Electrical Measurements

Supervisors:
Johan Nilsson (LTH)
Johan Gran (LTH)
Thomas Lawton (Axis Communications AB)

LUND
UNIVERSITY

Faculty of Engineering LTH
Department of Biomedical Engineering

Abstract

Electromagnetic compatibility (EMC) is a vital part of product development, and understanding the sources and causes of the emissions can facilitate tremendously in reaching compliance requirements and reduce the work needed for troubleshooting. At Axis Communications, where this thesis has taken place, the knowledge of EMC is an important part of their work and they aspire to improve further. This thesis aims to create a test setup and method to investigate one common interference source that can create challenges in the development of new products. Using the same method to identify and find solutions to common interferences facilitates the development process and reduces the need for EMI (Electromagnetic interference) troubleshooting. In the project, the electronics of one of Axis' cameras were investigated and tested through A/B tests, where new tests are formed by analyzing the results from the previously performed tests. The different types of testing that were conducted in the project were measuring the emissions in an anechoic chamber with varying changes made to the device under test, 'sniffing' with near field probes on the printed circuit boards (PCBs), and determining the resonant frequencies for cables with a network analyzer. The project results include identifying the source of one clock signal and its harmonics and characterizing the emissions from it depending on PCB placement and the surrounding material. The impact the slip ring made on the emissions was investigated and it was deemed not to affect them in any significant way. The investigation of the anechoic chamber and how the choice of cables used outside it could affect the zoning and cancel the shielding of it.

Acknowledgements

I want to thank everyone who has helped me through this thesis project and contributed to realizing it. First, I would like to thank my industrial supervisor Thomas Lawton for all the guidance and support throughout the work process and for making sure I had all the resources needed. Then I want to thank my academic supervisors Johan Gran and Johan Nilsson for the support and discussions helping me to move forward in my work and helping me learn more about my chosen field. The next thanks goes to Henrik Landahl and Claes Ingvert who with their broad spectrum EMC knowledge gave me a lot of ideas and help in analyzing test results and forming new tests. I would also like to thank my friend Lilly Abeln who has helped me review my report and correct my writing mistakes, my coworkers at Axis for their support, and of course Axis Communications for the opportunity to carry out my thesis with them. Lastly, I would like to thank my cat Samwise for all his hard work and all the support he has given me (motivating me to do my best and learn so that I can get a job in the future and pay for his food and home).

(a) Sam being motivating

(b) Sam working hard on the report

Figure 1: The author's cat Samwise working hard on writing the report.

Contents

List of Abbreviations

CAD	Computer Aided Design
CISPR	International Special Committee on Radio Interference
DUT	Device Under Test
EMC	Electromagnetic Compatibility
EMI	Electromagnetic Interference
FAR	Fully Anechoic Room
FSOATS	Free Space Open Area Test Site
GND	System Ground
IR	Infrared light
LED	Light Emitting Diode
LPDA	Log Periodic Dipole Array
OATS	Open Air Test Site
PCB	Printed Circuit Board
RF	Radio Frequency
SAC	Semi Anechoic Chamber
STP	Shielded Twisted Pair cable
UTP	Unshielded Twisted Pair cable

Introduction

1.1 Background

Electromagnetic compatibility (EMC) is a vital part of modern technology, as all products on the market must be compatible with the surrounding electromagnetic environment so that they don't interfere with or get interfered with by nearby electronics. However, achieving this is not so simple. There are a lot of components and subsystems that can cause interference and it is difficult to predict where conflicts may arise. A consistent and structured test setup and procedure can aid in this. It can help in the identification of interference sources in many different projects and products. Rectifying basic interference problems in components later used in many other products can reduce troubleshooting and workload down the line significantly. For many companies, such as Axis, where this thesis project has taken place, the work on EMC is very important, and with the constant development of new products the value of a good system for EMC testing and knowledge increases. Axis is a company developing products and network solutions for video surveillance, access control, intercom, and audio systems.

1.2 Project aim

To further the knowledge of EMC in its products and work on a more widespread testing approach, Axis's goal for this master thesis is to investigate common EMC challenges that may arise in the development of its products and how to resolve them. This is done by investigating the electronic design of one of its cameras. The aim of this project was divided into three parts.

- Construct a test setup for the chosen camera and the camera components that are of interest.
- Bring forth a testing plan and method to identify interfering sources and investigate them.
- Use this plan and method to identify a common interfering source and investigate it.

The test plan and method should be designed in a way that can be applied in the testing of various products and subsystems. Providing a uniform way of testing makes the testing process more efficient and consistent throughout different projects, reducing development time and helping maintain high-quality standards.

1.2.1 Project limitations

Because of the scope and the investigatory nature of the project, the constricting factor will be time, and whether or not all the characteristics of the interfering source are identified depends largely on the problem itself. Therefore the decision was made to define an end date for the testing phase and use that for one of the project limits. This limitation also contributed to the decision to focus on identifying and characterizing the source of one common EMC issue for radiated emissions between the frequencies 30MHz and 1GHz. Further limitations are the available equipment and what kind of tests can be performed with, for example, the available 3 meter anechoic chamber and the measuring instruments like spectrum analyzer, test receiver, and network analyzer. Lastly, no large changes will be made to the electronics of the device under test, for example, changing the layout of the PCBs is not possible with the time and resources at hand.

1.3 Report disposition

After the introduction, the report goes into and explains the theory being used in the project, including a basic introduction to EMC, the measuring equipment and compliance requirements, and an antenna overview. Following this is the Method where the test rig and procedures are described and explained together with the execution. Next is the result and discussion. In the result all results of the testing are presented, and in the discussion, the results are analyzed together with whether the thesis goal was reached, possible improvements, and further research. Lastly, ending the report with a conclusion summarizing the findings, followed by references and an appendix.

Theory

2.1 Introduction to EMC

To understand EMC (electromagnetic compatibility) we need to understand the concept of electromagnetic interference (EMI) since this is what occurs when EMC is not achieved. There are three components needed for EMI to exist; a source, a victim, and a coupling path between the source and victim [1, p. 2]. This project will focus on the source and the emissions from it.

2.1.1 Sources of interference

All electronics emit electromagnetic emissions. Where there is a change in current there will be a magnetic field, and where there is a change in voltage there will be an electric field. However, for interference to occur there needs to be a coupling path to a victim affected by the emissions.

Focusing on the source of the emissions there are a lot of practices to minimize the emissions so they do not become interferences, everything from how to route signals and implement the ground properly to minimize the field strength in the electromagnetic fields, to shielding and filtering signals to disrupt or cut off the coupling path at the source.

2.1.2 Coupling

The coupling between source and victim can occur in various ways, the most common is through proximity, radiation, or a direct connection. The different connections are explained below.

Direct coupling

The easiest to visualize is often the direct coupling, where a direct connection exists between the source and the victim. This can happen via signal or power lines or through a common impedance coupling. For example, if there is a disturbance present on the port of a power supply or a signal line the disturbance will propagate through the wire to the port of the victim. An example of a common impedance coupling is when two separate systems are connected to earth through the same busbar. The internal noise-current from the source is connected to ground through the busbar, and because of the actual impedance of the wire, this current creates a difference in voltage between the busbar and the busbar's connection to earth. The

victim who also is connected to earth through the busbar is now directly coupled to the noise.[2, pp. 78–80]

Near field coupling

Interference through proximity, or near field coupling, is either inductive or capacitive and the definition for what is considered near field is within the distance of $\lambda/2\pi$ from the source. Inductive interference is the result of when the magnetic field created by the current in a conductor induces a current in another conductor. The voltage induced in a victim conductor by a current is given by equation 2.1, where M is the mutual inductance and i is the current in the source.

$$V_N = -M * di/dt \tag{2.1}$$

Capacitive interference occurs because of the electric field that is created between two conductors of different voltage potentials. The induced voltage on the victim conductor from the field is given by equation 2.2

$$V_{in} = C_C * Z_{in} * dV_S/dt \tag{2.2}$$

where Z_{in} is the impedance of the victim, V_S the interfering voltage and C_C the mutual capacitance.[2, pp. 81–84]

Radiated coupling

When the distance from the emission source has reached $\lambda/2\pi$ the emissions are classified as radiated. At this distance, the electric and magnetic fields are no longer considered separate from each other since a varying current causes the voltage to change and fluctuation in both current and voltages will produce both magnetic and electric fields. At this distance from the source these fields will resolve themselves and their corresponding vectors will be perpendicular towards each other and the direction of propagation. The interference can now be visualized as a plane surface radiating outwards from the source and the propagating wave interferes with the victim by inducing voltages and currents similar to if the source was an antenna. [2, pp. 84–85]

2.1.3 Common-mode and Differential-mode

In EMC an important aspect to understand is the modes of coupling, common mode, and differential mode. The modes of coupling rely on the idea that two different circuit paths can exist in the same set of conductors. The differential mode is where the signal and return current, or power and return flows as intended by the designer in opposition to each other. The other, common mode, is where the current flows in the same direction in the conductors with the return in an unintentional part of the structure which the circuit is located in. This could, for example, be the safety earth or external structure. In figure 2.1 the different modes are illustrated with the common mode return current coupled parasitically.

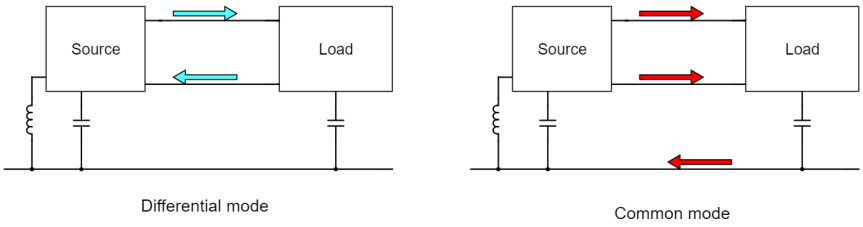

Figure 2.1: Illustration of Common and Differential mode. Where the arrows represent the current flow. The conductor at the bottom of the picture represents an external structure parasitically coupled to the source and load.

2.1.4 Zoning in EMC

The concept of zoning in EMC is to have different levels of EMC protection for different parts of a system. This is often done to protect sensitive parts of a device or system. Between zones there will be some kind of barrier or protection separating the different electromagnetic environments from each other, like shielding and the use of filters, it can also be that the earthing system is more controlled. The use of the zone can be to protect the inside from the outside environment as well as the outside from the inside environment. For example, a chamber used to measure the EMI of different products needs the electromagnetic environment in the zone inside the chamber to be protected from the noise in the zone outside. However, for some equipment with high electromagnetic emission, the equipment can be placed in a shielded zone, protecting the outside from the noise emitted by the device.

The number of zones used is most commonly 2 or 3, but in special cases, there might be a need for more than that. The surrounding environment is often referred to as zone 0, ie the setting where the system or device is placed. Then the next zones are zone 1 and zone 2, increasing in protection with a higher number. [2, pp. 90–91]

2.1.5 Grounding in PCBs

To minimize the radiated EMI or RF energy from a signal path in a circuit it is important to have a well-implemented ground where the signal return path is closely coupled to the signal. When the RF signal trace and its return signal are in close proximity to each other the magnetic flux gets canceled out because of their opposite polarisation, thus reducing the emission. This is most often achieved with RF return planes, also called image planes, where the return current can image back along its source in differential mode. If a two-wire transmission line is slightly unbalanced it will create higher levels of common mode radiated emissions than that of the differential mode radiation from the closed loop. [3, p. 92] [4] [5]

Since the return current most often flows through the ground, the ground is implemented as a plane parallel to the signal paths. This is called the ground plane. For maximum magnetic flux cancellation, the ground plane can not be broken by any gaps or slots in the conductive material. This creates concerns when layer jumping which refers to a signal switching layers in the printed circuit

board. When this happens the signal will most likely also change which ground plane it is closely coupled to, and so creating a gap in the ground plane. To combat this gap in the ground plane the two ground planes have to be connected through one or more vias tightly coupled to the signal via, to keep the return current close to the signal current in differential mode. If not, unwanted common mode currents will likely develop. This is especially important for high-bandwidth signals like clocks, video and address lines, and analog circuits. [3, pp. 96–99] [6]

2.1.6 Ferrite beads

Ferrites are used to filter away unwanted magnetic fields. When a time-variant current flows through a conductor a magnetic field is created around that conductor. Normally the material around that conductor is non-permeable like air and plastic and the magnetic field strength and flux density are equal. However, when placing a ferrite whose material is magnetically permeable around that conductor, the magnetic flux density of a given field strength will increase, and the inductance of the wire will increase. The magnetic flux density is dependent on the permeability of the ferrite and changes based on the composition of the different oxides used to construct it, making it frequency-dependent. [3, pp. 295-298] The ferrite around the conductor will only affect the common mode current and not the differential mode current because of the cancellation in the magnetic field around the adjacent differential mode conductors. While the common mode current generates a net magnetic field around the conductor, causing the ferrite to increase the cables' local impedance as described above for the common mode current, the differential mode currents do not, and will therefore not be affected by the ferrite. The attenuation of a ferrite on a conductor is usually around 6-10dB since the ferrite generally only adds a couple of hundred ohms inductance to the wire. The attenuation can be higher for frequencies where the cable shows low inductance, reaching around 20dB as a result of the greater proportional change in impedance. [2, pp. 208–209]

2.2 Measuring

When measuring electromagnetic interference it is important to know about the equipment used and the surrounding environment. There are a lot of factors that can affect the measurements such as how the equipment works and its limitations, what material the table being used is made of, and if there is a ground plane nearby affecting your measurements.

2.2.1 Compliance requirements

When doing compliance requirement testing, the measurements have to be conducted in certain ways and environments. The standards specify amongst other things what cables must be used and how to physically arrange them in the lab/test site as well as many more specific details. All these requirements are necessary to ensure an environment without any other interference and to minimize reflections. For radiated emissions a test site called OATS (Open Area Test Site) is to be used, it is specified that the site must have an interference-free area around the device under test (DUT) and the antenna as well as be completely free from any material

that can reflect Radio frequency (RF) waves. The only exception to this is the unavoidable ground plane that instead has size conditions.

For most standards, conducted emission is measured from 150kHz to 30MHz and radiated emissions from 30MHz to 6GHz.[7, pp. 273–274] There are a lot of different standards depending on the type of product and in what environment it is intended for, there is class A for industrial environment and class B for residential environment, where class B have a lower limit for how much the device is allowed to radiate and how much it can handle from the surrounding. In table 2.1 the requirements for the device in industrial use (class A) for emissions under 1GHz are presented and in table 2.2 emissions over 1GHz are presented. In the tables are the terms peak, quasi peak, and average used. These are different detector functions and are explained in section 2.2.6.

Table clause	Frequency Range MHz	Measurement			Class A limits dB ($\mu V/m$)
		Facility	Distance m	Detector type/ bandwidth	
A2.1	30 to 230	OATS/ SAC	10	Quasi Peak/ 120kHz	40
	230 to 1 000				47
A2.2	30 to 230	OATS/ SAC	3		50
	230 to 1 000				57
A2.3	30 to 230	FAR	10	Quasi Peak / 120kHz	42 to 35
	230 to 1 000				42
A2.4	30 to 230	FAR	3		52 to 45
	230 to 1 000				52

Table 2.1: Requirements for radiated emissions for class A equipment below 1GHz. [8]

Table clause	Frequency Range GHz	Measurement			Class A limits dB ($\mu V/m$)
		Facility	Distance m	Detector type / bandwidth	
A3.1	1 to 3	FSOATS	3	Average / 1 MHz	65
	3 to 6				60
A3.2	1 to 3			Peak / 1 MHz	76
	3 to 6				80

Table 2.2: Requirements for radiated emissions for class A equipment above 1GHz. [8]

2.2.2 Anechoic Chamber

An anechoic chamber is used to mimic an open area test site. This is a room or chamber that is fully shielded from RF emissions. The walls and roof on the inside of the chamber are covered with a ferrite material and cones of radiation-absorbent material to remove RF reflections inside the chamber. The ferrite material stops the lower frequencies from reflecting and the radiation-absorbent cones stop the higher frequencies. No metal or conductive material apart from the DUT is allowed in the chamber and the table used to place the device under test on, is most often made out of styrofoam or wood.

2.2.3 Network analyzer

A network analyzer is an instrument that measures the characteristics of an electrical RF network. Because it is hard to measure the currents and voltages for RF frequencies, the network analyzer uses a method where it sends a known signal into the device under test and measures the ratio between the input and output signal. Using this method, the network analyzer measures the device or network's behavior over different RF frequencies. The early network analyzers, called scalar network analyzers measure only magnitude like return loss, gain, and standing wave ratio. The newer network analyzers called vector network analyzers can measure phase as well, making them very versatile and can for example characterize a variety of parameters, make time-domain measurements, and match complex impedances. [9]

2.2.4 Spectrum analyzer

One of the most common testing devices within the field of EMC is the spectrum analyzer, it is widely used for diagnostics and quick testing. It has an instantaneous spectrum display which is highly useful when confirming emission frequencies, and the ability to zoom in on a narrow part of the spectrum further improves this quality. The spectrum analyzer, nevertheless, has some limitations. The input signal of the analyzer is directly connected to a mixer covering the entire frequency range making the spectrum analyzer noise sensitive, and interesting signals can get lost in the noise floor. The mixer is a very sensitive component and connecting the input directly to it can easily damage the spectrum analyzer due to transients on the input. The mixer can also get overloaded by broadband signals making it cross over to non-linearity which will lead to inaccurate readings without any indication of such.
When using the spectrum analyzer it is important to know that it includes the time domain as well as the frequency domain since it sweeps through the frequencies which takes time. Broadband short pulses can thus appear to only be at discrete frequencies when looking at a single picture of a reading. [7, pp. 141–142]

2.2.5 EMI test receiver

The EMI test receiver is very similar to the spectrum analyzer and they are often used interchangeably with each other. However, it is important to know the differences between them and when they can not be used in each other's staid. One of the main differences is that instead of using a continuous sweep like the spectrum analyzer, the test receiver performs a stepped sweep when measuring the spectrum. The instrument is tuned to specific frequencies with a set step size between them, building up the entire spectrum. The EMI test receiver also has a built-in preamplifier, lowering the noise floor and giving the EMI receiver a higher capability of picking up signals otherwise lost in the noise.

Other things that the spectrum analyzer can be short of compared to the EMI test receiver are for example the ability to conduct quasi peak measurements (described in section 2.2.6) and preselection filtering. Most spectrum analyzers use a Gaussian-shaped filter which might not meet the compliance requirement standards. [10]

2.2.6 Detector functions - Peak, Quasi-peak, and average

Since interfering emissions are rarely constant at a certain level and can among other things be pulse or amplitude modulated, there is a need for different ways of detecting and measuring emissions. Commonly used are the three detector types peak, quasi-peak, and average.

Peak

Peak detectors display the peak value of the emission signal almost instantaneously, and then get discharged fairly quickly. This is practical for quick and easy first diagnostic measurements and can reduce the time needed for compliance measurements later. However, it is hard to determine the effect of the disturbance through this test since it does not consider the repetition frequency of the emitted signal. Below 1GHz there are no requirements from the CISPR emissions standards for this type of test.

Quasi-peak

The quasi-peak is a weighted peak detector. The quasi-peak takes into consideration the frequency in which the pulse is repeated, for instance, a pulse reappearing with a high frequency has a higher disturbance. The quasi-peak always displays a lower value for pulse-type emissions than the peak detector. When making the quasi-peak measurements the detector must dwell on each frequency for several charge and discharge cycles for an accurate reading, making the measuring time substantial.

Average

The average detector registers the average value of an emission signal, this value is always less than or equal to the peak value and is only equal for a continuous signal. The average limit on CISPRs emissions standards for conducted emissions is 10-13dB lower than the limit for quasi-peak measurements. [7, pp. 145–146]

2.2.7 Near field probes

To locate the physical source of emissions near field probes are used, also called sniffer probes. As the name suggests the near field probes detect emissions in the near field. Because near field coupling is either inductive or capacitive there are two types of near field probes, one for detecting electric fields and one for detecting magnetic fields. They are both very simple and can be fabricated using a coax cable. The E-field probe can be created by leaving a short unshielded part at the end, and an H-field probe by making a loop at the end leaving a gap in the shield either at the loop connection or the loop's halfway point for an improved H-field probe.

The probe sensitivity and spatial accuracy depend on the probe dimensions. A small probe will have a higher accuracy but lower sensitivity, and a bigger probe higher sensitivity but lower accuracy.[7, p. 163]

2.2.8 A/B test

A/B testing is when two or more tests/measurements are conducted where only one aspect is changed between the different measurements. This is to be able to compare the resulting measurements against each other and see the effect of the change made. First, a baseline is measured, test "A", then one adjustment is made to the DUT (or setup), and another measurement is made, test "B". Comparing test "A" against test "B" can then reveal characteristics of the device under test and increase knowledge and understanding about the DUT.

2.3 Antennas

An antenna is an electrical circuit where, unlike most others, the circuit's size is close to or equal to the wavelength in which it is operated. This allows for the energy in the circuit to escape in the form of electromagnetic waves, thus creating the antenna. The closer the length of the antenna is to a multiple of $1/2\lambda$ the greater the radiated field will be for the wavelength λ. [11, p. 2-1] And vice versa, an electromagnetic field will induce a current in a conductive material if the length of it is proportional (1/2 multiple) to the wavelength.

2.3.1 Antenna factor

When doing measurements with an antenna it is important to know what the antenna factor is. The antenna factor is the frequency-dependent ratio between the electric field strength and the induced voltage over the terminals of the antenna. It is a way to weigh together directivity and effectiveness. For example, to get the correct field strength from what is measured with the spectrum analyzer, the antenna factor needs to be added to the measurements along with cable loss and other attenuation and gain factors.

2.3.2 Antenna Gain and Directivity

The radiation from an antenna is never the same in all directions and thus exhibits directive effects, this is called the directivity of the antenna. The directivity of an antenna is derived by comparing the 3-dimensional pattern of the antenna with the 3-dimensional pattern of an isotropic antenna, an ideal antenna where the field strength is the same all around the surface of a sphere with the antenna at the center. Taking the maximum power P of the same sphere around the actual antenna radiating the same total power as the isotropic antenna and dividing it with the average power density P_{av} gives the directivity D. The calculation of the directivity of an antenna can be seen in equation 2.3.

$$D = \frac{P}{P_{av}} \tag{2.3}$$

The antenna gain is a parameter that combines the radiation efficiency and the directivity, the antenna gain can be seen in equation 2.4

$$G = k\frac{P}{P_{av}} \tag{2.4}$$

where k is the efficiency of the antenna, which is defined as power radiated divided by power output.[11, p. 2-22] [12]

2.3.3 Radiation pattern

An antenna's radiation pattern is a graph showing the field density as a function of the direction away from the antenna. This field density can be either the actual value or a relative value, and the graph can be represented in different ways. The graph can be 2-dimensional or 3-dimensional and different scales can be used, for example; linear grid, log periodic grid, and logarithmic (linear decibel) grid. Often a log periodic grid is used and in figure 2.2 a 2-dimensional radiation log periodic pattern is shown in A and a 3-dimensional pattern in B.[11, pp. 2-12–2-16]

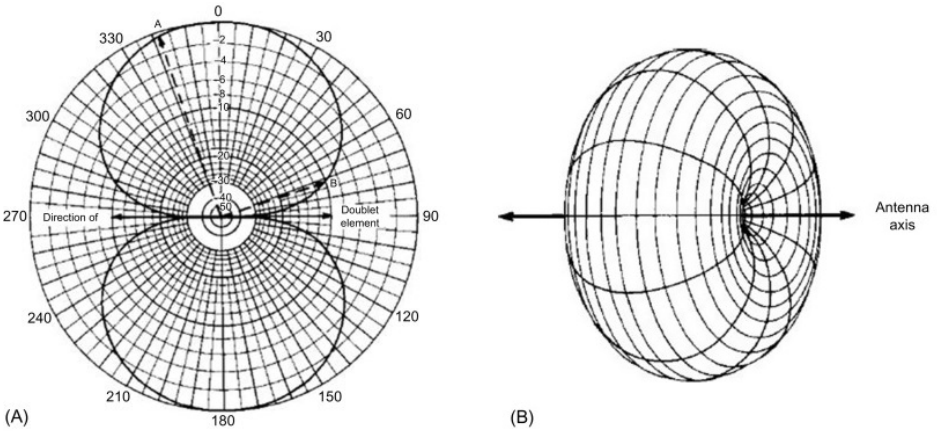

Figure 2.2: Radiation pattern of a half wave dipole (described in section 2.3.4, logarithmic scale. A is the 2-dimensional pattern and B is the 3-dimensional pattern. Adapted from [13]

2.3.4 Dipole antenna

The dipole antenna is an antenna that has its driving element in the center creating two poles.[14, p. 150] Driving the antenna with high frequency voltage equal to its resonant frequency creates a standing wave of electrical and magnetic fields over the length of the antenna [15], resulting in the radiation pattern seen in figure 2.2. When first learning about antennas most people learn that the length of an antenna is equal to half the wavelength of the frequency we want the antenna to be optimal and resonant at, however in reality this is not quite right. The physical length of the antenna is always somewhat shorter than its electrical length, which is the length determining the resonant frequency. The physical length of the antenna depends on the ratio between the length of the conductor and its diameter. For an antenna made of wire, the physical length of a half-wave antenna is about $0.98\frac{\lambda}{2}$, but by increasing the width, the length shortens. The average antenna length is around 95-98% of the half wavelength.[11, p. 2-3]

2.3.5 Log periodic antenna

The log periodic antenna is an antenna that can be operated over a wide range of frequencies, it is built up through a system of driven elements. There exist many different varieties of log periodic antennas, most commonly known and used is the log periodic dipole array (LPDA). For the LPDA the driver is placed between the smallest elements at the front of the antenna. The longest element at the back end decides the lowest frequency for which the antenna is designed, with its length being a half wavelength of this frequency. The operating frequency is most commonly 200-1000MHz. Over the LPDA's frequency range its electrical parameters, such as feed-point impedance, gain, and front-to-back ratio stay more or less the same. This is a unique feature for the LPDA. [11, p 10-1]

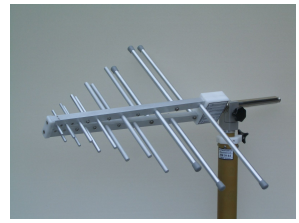

Figure 2.3: Log periodic dipole array [16]

2.3.6 Biconical antenna

Figure 2.4: Biconical antenna [17]

The biconical antenna is developed from the half-wave dipole with the elements formed in a conical shape, which increases the operating bandwidth for the antenna while maintaining the same directional properties as the dipole. For EMC measurements the operating frequency for the biconical antenna is often chosen to be 30MHz to 200MHz or 30MHz to 300MHz. The biconical antenna is often made as a skeletal structure like the one in figure 2.4, to minimize weight and wind resistance while maintaining the properties of the antenna. [2, p. 245]

2.3.7 BiLog antenna

The bilog antenna is essentially a log periodic and biconical antenna combined, allowing the spectrum from 30MHz to 1GHz to be measured with the same antenna. This is very practical when compliance measuring since there is no need to switch the antenna during measurements, which otherwise adds concerns connected with changing the setup and damaging connectors etcetera. [2, p. 246]

Method

In this chapter, the execution of the project is presented and explained. Firstly the testing approach, the equipment, and the device under test are defined and explained, then follows the execution going through how the measurements and tests were done and how they were motivated.

3.1 Equipment

Spectrum Analyzer Keysight N9322C

Network Analyzer Advantest R3767CH

EMI Test Receiver 6GHz Rohde & Schwarz ESL6

Shielded twisted pair cables

Near field probes Constructed from coaxial cables.

EMC32 Software by Rohde & Schwarz for collecting measuring data and control measuring equipment

Anechoic chamber With turntable and bilog antenna

3D printer Creality um2 and um3

Ferrite beads Type 742 711 32, datasheet in appendix B

3.2 Testing approach

When doing EMC testing in search of emission sources it is nearly impossible to settle on a complete plan beforehand, since the tests needed will change with every new device. One cannot precisely predict what emissions will occur. An experienced person in EMC can have a good idea, but only testing will reveal the test unit's actual interferences.

To not be completely lost however, especially when new to EMC, using a testing plan or guide is important.

The testing approach used in this project is an investigatory testing approach where, through analyzing the previous test results, new comparative A/B tests are formed. Individual changes are made to the DUT or test setup and the results are then compared between test A and test B to find out new information and

characteristics of the DUT, help confirm or deny hypotheses, and/or narrow down where the interferences derive from. The goal of these testing procedures is to identify the sources of emission and how the signals propagate through the device and radiate from it. The developed and used method is visualized in figure 3.1.

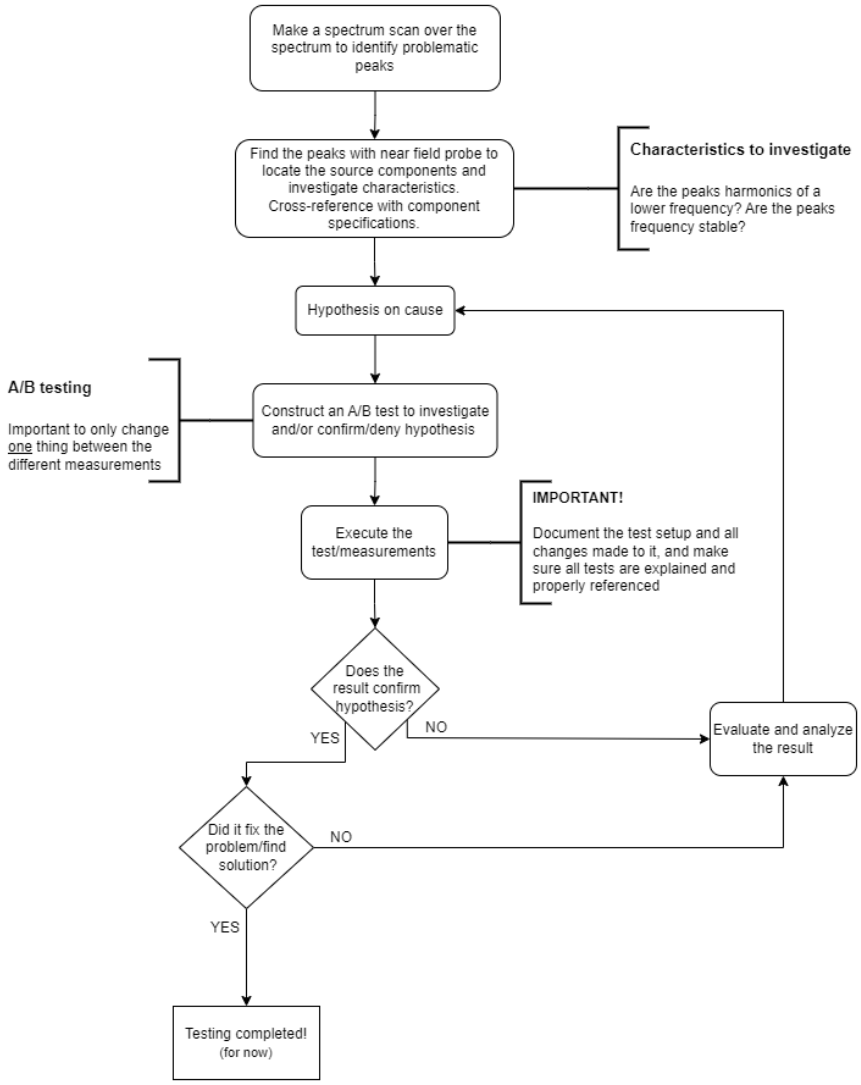

Figure 3.1: Flowchart of the developed test method.

The testing approach also involves different methods of testing, namely measuring with an antenna in an anechoic chamber, measuring with near field probes, and looking at frequency resonances with a network analyzer which is further explained in section 3.6.

3.3 Anechoic chamber test setup

The radiated emissions tests were executed in an anechoic chamber. An anechoic chamber is a chamber that represents an open area test site (OATS) and is therefore shielded from outside noise, has a ground plane on the floor, and has a low degree of reverberation.

The Anechoic chamber used has a Bilog antenna connected to an EMI test receiver and a turntable 3m from the antenna. This is all controlled from outside of the chamber with the program "EMC32". Through this program, the antenna polarisation and turntable positions are controlled and all measurements are made. Measurements can be done individually or through an auto test, taking approximately one hour to execute, where the program goes through and measures the spectrum for eight table positions (0, 45, 90, 135, 180, 225, 270, and 315 degrees) and the two antenna polarisations vertical and horizontal, resulting in 16 measurements from where the worst peaks are merged into one final result. All measurements are peak measurements and are done with a bandwidth of 120kHz, dwell time of 10ms, and step frequency of 40kHz.

To minimize the impact of the connected Ethernet cable depending on the table position, a hole was made in the table to put the wire through making it go directly from the DUT straight down to the floor connection. In the chamber, a shielded twisted pair cable is always used if nothing else is specified.

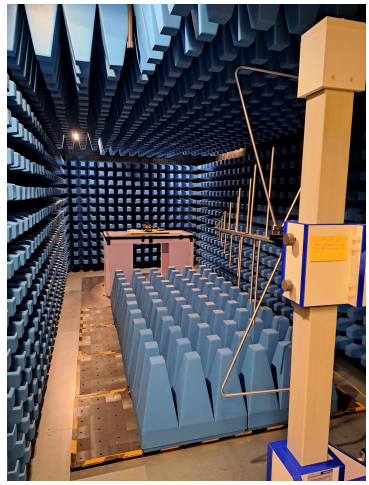

Figure 3.2: The anechoic chamber with DUT

3.4 DUT - PCBs

The device under test is the electronics part of the camera, consisting of a power PCB connected through a slip ring to the main PCB which in turn is connected to the camera block through two wires. The camera block consists of the camera optics, lens board, sensors, and other components. A slip ring refers to cables with a mechanical part where the two sides can revolve around each other without getting twisted or losing the connection between them. A picture of the slip ring can be seen in figure 3.9a. The device is powered through and communicates over

an ethernet cable connected to the power board. Testing will also be conducted on the full camera product which will be referred to as the whole camera.

Firstly a testing setup for the chamber tests needs to be constructed. To make it possible to execute identical tests in the test chamber it is important that the DUT can be placed in the exact same way for each test, with the connecting wires in the same position. This is done by getting the exact measurements of the DUT to create CAD models and 3D-print stands for the different parts, namely the PCBs, the camera block, and holders for the wires. These stands are then screwed onto a wooden slab to be placed on a turntable in the chamber. The placement on the table is marked to be consistent for every test. The choice to use a wooden slab and 3D-print holders for the different parts is to not affect the measurements with any conductive material. The screws are made of metal but were deemed small enough not to affect the measurements.

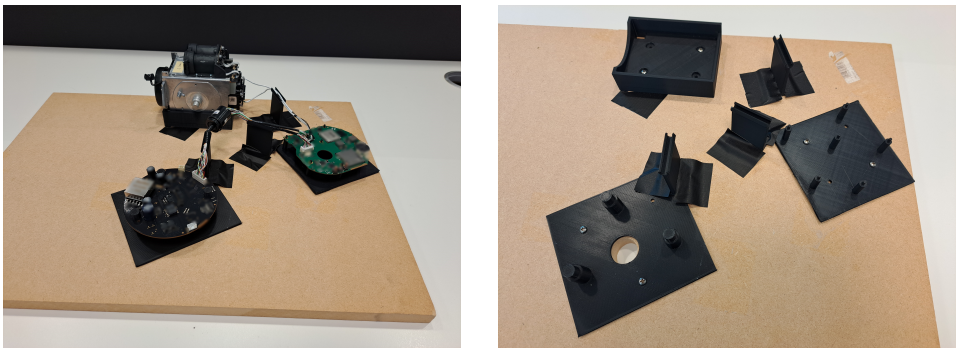

(a) **(b)**

Figure 3.3: The DUT and its setup with the 3D printed holders on the wooden slab. In Figure B are the holders on the slab and in Figure A the PCBs and camera block are placed on the holders.

3.4.1 Devices used in tests

PCBs The PCBs as described in section 3.4 and pictured in figure 3.3a. Measured both on the setup as well as in other configurations.

Camera 1 A whole camera, later discovered to be an earlier version from the other DUTs

Camera 2 A whole camera

Camera 3 A whole camera

Camera 4 A whole camera

3.4.2 Cable configurations

For the ethernet cable and ground cable connected to the DUT inside the chamber three different configurations of their placement were used during testing. These different configurations are presented in figure 3.4. First is the ethernet cable without ground cable, then two configurations with both ethernet and ground cable, one with them separate and one where they are twisted together and pulled

through the table straight to the floor. The default setup is with the ethernet cable straight down through the table as shown in figure 3.4a, and this is what has been used if nothing else is specified.

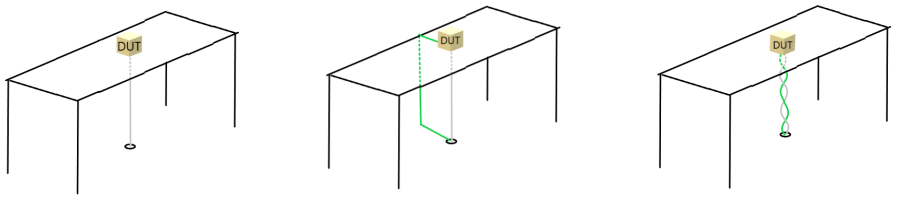

(a) Ethernet cable straight down through the table.

(b) Ethernet cable straight down through the table and ground cable hanging of the side of the table.

(c) Ethernet and ground cables twisted together pulled straight down through the table.

Figure 3.4: The different cable configurations used in the tests.

3.5 Initial testing

The first step of testing the PCBs is a peak scan over the full spectrum in the test chamber to identify problematic frequencies. This is done for eight table positions at 45° intervals between each position and two array angles for each position; horizontal and vertical, resulting in sixteen spectrum scan measurements in total. A compilation of the highest peaks from all positions is shown in figure 3.5.

The next step is to identify the location of the emission source on the device. This is done with sniffing with near field probes and the spectrum analyzer. Here it's important to investigate the lower frequencies that can be a denominator to higher frequencies. Sniffing is done by carefully going over the top and bottom layer of the PCBs with a small near H-field probe assessing what frequencies were found and where, and at the same time cross-referencing with the schematics and layout, identifying what sources the different signals are coming from. This is done for the whole frequency span, with the bandwidths 9kHz for the 0.15-30MHz frequency range and 120kHz for the 30MHz-1GHz frequency range. Zooming in on the detected signals reveals information about whether they are frequency-stable or not.

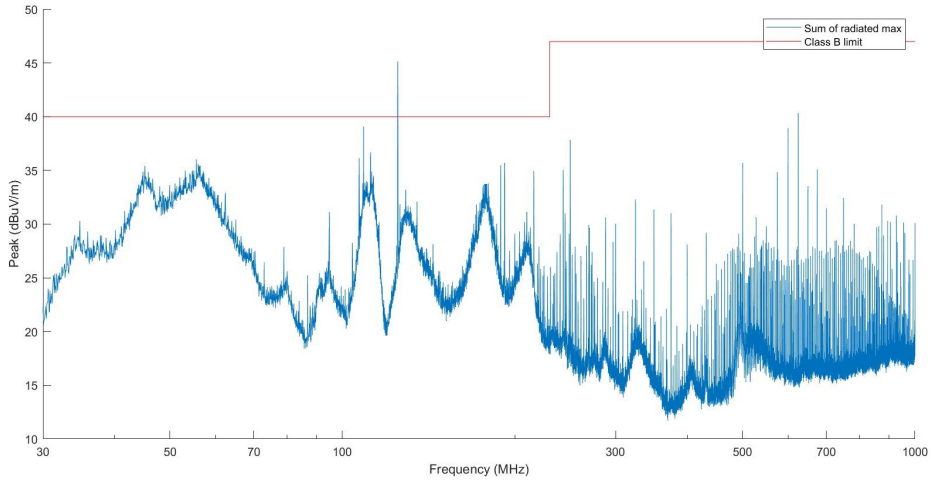

Figure 3.5: Initial spectrum scan of the emissions from the PCBs on the 3D printed holders. The result is a compilation of the highest peak values from all directions and the antenna polarizations horizontal and vertical. The figure includes the limit line for Class B compliance requirements.

3.6 Method testing

To decide which of the testing approaches and different methods could be used, some experiments were conducted with a variety of possible test methods.

An examination of the existing resonances in the cables was done with a network analyzer and an H-field probe connected to the measured wire through a ferrite. The difference in resonance depends on the circuit itself but also the properties of everything connected, both physically and through proximity making the connections between the surrounding structures and the placement of the PCBs in relation to each other affect the resonances. This is something that was lightly explored to increase understanding and enhance the feeling of placement importance.

3.7 Execution

In this section, the different tests are explained and motivated. Most of the tests done are derived from earlier test results and therefore will refer to results in chapter 4. Furthermore, the resulting data from the measurements were exported from the measuring software to Matlab to be plotted and analyzed there. An example of the Matlab code that was used can be viewed in appendix A.

From the initial spectrum scan a 125MHz signal and its harmonics were prominent, and from sniffing with near field probe, the origin of the signal was deduced as stated in section 4.1.1 of the results. This signal is a vital part of most applications and can cause difficulties when compliance testing. This motivated the decision to focus on the 125MHz signal and its harmonics to test the testing approach and learn more about how and what makes this signal radiate and become a disturbance.

3.7.1 Resonance and Emission from connecting wires

To investigate what components on the DUT are acting as an antenna the radiation from the various cable connections between PCB boards and the camera block were examined. Measurements of their resonant frequencies were made with a network analyzer, and A/B tests of the impact of ferrite beads on the different connections were conducted using the chamber setup. The A/B tests were done with the table in position 0°. A baseline without ferrites was first measured, then two 742 711 32 ferrites were placed on the cables between the main board and the camera block, and new measurements were made. These measurements were repeated with the ferrites on the cables between the main board and the slip ring as well as with the ferrites between the slip ring and the power board. The placements of the ferrites are shown in figure 3.6, and the results from the tests are presented in figure 4.2. Looking at the results in figure 4.2a we can see that the ferrites do not have an impact on the 125MHz signal and its harmonics when placed between the camera block and the main board. Therefore it is unlikely this path is taken by the signal and is not the source of radiation. Looking at the results in figure 4.2b and 4.2c there is a significant dip in amplitude for the frequency 125MHz and in figure 4.2b dips in higher frequencies as well.

For a better overall result with information about the emission from all directions, the test was repeated with an auto test going through horizontal and vertical polarization for the eight directions used, summarizing a final graph for all measurements. These results are shown in figures 4.3, 4.4 and 4.5, and is summarized in table 4.2.

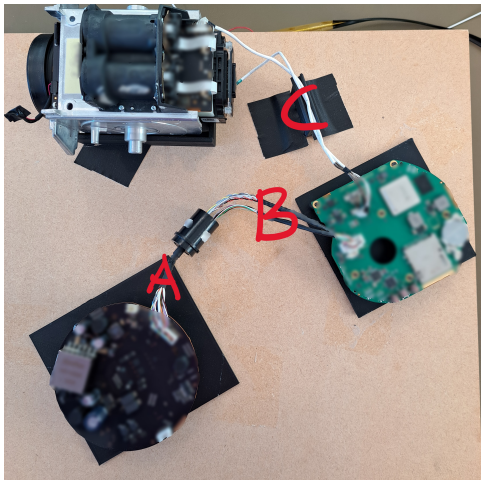

Figure 3.6: The DUT with the cable connections marked with A, B, and C for where the ferrites were placed. A is between the Power board and slip ring, B is between the main board and slip ring, and C is between the main board and the camera block.

3.7.2 Whole camera vs PCBs

The whole camera consists of many more parts than only the PCBs and camera block. Due to this, testing on bare PCBs may not resemble the product since surrounding materials and placement have a large impact on the results. To identify possible implications, testing was conducted with the whole camera as well as the

PCB test setup. Measurements were done in all eight directions for both vertical and horizontal polarisation for the whole camera and the PCBs. The results can be viewed in figure 4.6. The camera tested was camera number 1, which was later discovered to be an earlier version of the camera from which the PCBs are from. The cables connected to the camera were the ethernet cable straight down through the hole in the table and a ground cable placed on the table and hanging off the side as illustrated in figure 3.4b. This unusual cable setup was due to complications with placing them together through the table hole.

3.7.3 Sandwich test

Looking at the results comparing the whole camera and the PCBs in figure 4.6 and to draw any conclusions there is an interest in continuing to investigate what parts of the construction contribute to the emissions. To analyze the impact of the PCBs placement in relation to each other inside of the actual camera an A/B test, later named "sandwich test" was done. With the help of some plastic foam and some sticky tape the PCBs and camera block were sandwiched together in a similar way to how they are sitting inside the actual camera. A picture of the construction can be seen in figure 3.7, and a visualization of the placement of the different parts can be seen in figure 3.8. The measurements were done in horizontal and vertical polarisation for all directions and the results can be seen in figure 4.7 and 4.8 compared to the whole camera and the bare PCBs spread out respectively.

Figure 3.7: The PCBs and camera block are placed similarly to their placement inside the whole camera with the help of plastic foam and tape.

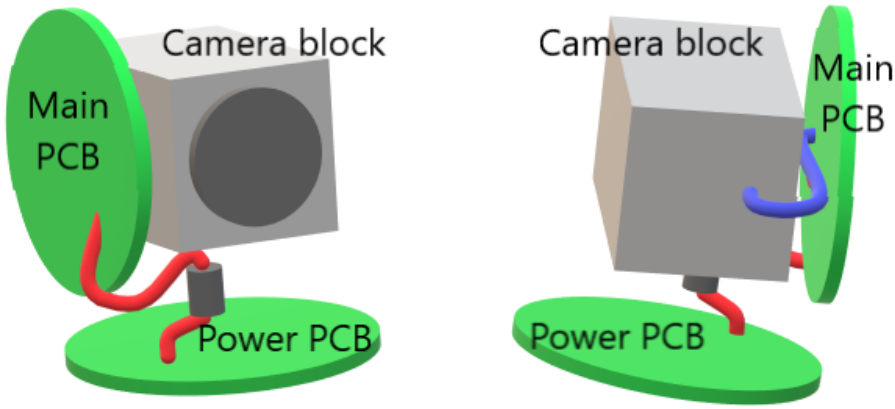

(a) The front of the camera

(b) The back of the camera

Figure 3.8: Illustration of the placement of Power PCB, main PCB, and camera block in relation to each other for the sandwich test.

3.7.4 Comparing whole cameras

Looking at the measurements from the whole camera in figure 4.6 there are multiple peaks around 100MHz that are not seen when measuring on the free PCBs. To see if this occurs for every camera, the emissions from two more whole cameras were measured. The results of these measurements that are shown in figure 4.9 can however only be used for drawing initial hypotheses and not for any conclusions. The measurements have been made on two different occasions and it can not be ensured that all parameters are the same. A known difference was that cameras 2 and 3 had the IR LEDs disabled while camera 1 did not. The results can indicate that more thorough testing is of interest.

Because of the importance of a well-implemented ground, tests were done where the contact spring connecting the chassis ground with the power board was bent to better the connection, giving the before and after measurements in figure 4.10.

The initial tests of the whole camera units as seen in figure 4.9 showed big differences between the cameras that were tested on different occasions giving incentive to continue examining the differences with more precise testing. Making sure all parameters were the same for all measurements, the measurements of camera 1 and camera 3 were redone, this time twisting and taping the ethernet and the GND cable together and pulling them through the hole in the table as shown in figure 3.4c. Giving the results in figures 4.11.

When analyzing the result in figure 4.10 of the before and after the improvement in the ground connection between chassis and power board the question of whether this big difference is unanimous for all cameras or if it was an isolated incident arose. The test was remade with cameras 3 and 4 with the improved setup with ethernet and GND cable twisted together as illustrated in figure 3.4c. Camera 4 was also tested with the contact spring removed and the results are presented in figure 4.12 and 4.13.

3.7.5 Investigating the setup

Re-taking the measurements of camera 1 revealed a significant discrepancy between the measurements made with the same camera on two different occasions as seen in figure 4.14. This and the fact that a lot of these differences could be seen for the frequencies of FM radio, the question of the setup quality arose.

To investigate if any interfering signals from outside of the chamber were leaking into the chamber, measurements were done where a whole camera was connected inside the chamber but not powered on. Measurements with different combinations of the connected cables on the outside of the chamber can be seen in the result figures 4.15, 4.16 and 4.17. Combinations with unshielded twisted pair (UTP) and shielded twisted pair (STP) cables connected to the different outputs of the chamber and through that ether UTP or STP cables inside the chamber. The cables outside the chamber were also tested open-ended or with a non-powered midspan connected.

3.8 Slip ring testing

To answer the question of how much the slip ring affects the emissions, first, the measurements to compare four different slip rings were made then the comparison between slip ring versus cables without the slip ring. The PCB setup was used and measured with the auto test for the four slip rings then one of the slip ring cables was converted into cables without the slip ring part and the measurement was redone with the modified cable. The slip ring cable was converted by cutting the slip ring part off and soldering together the corresponding wires. The results are presented in figure 4.18 and 4.19.

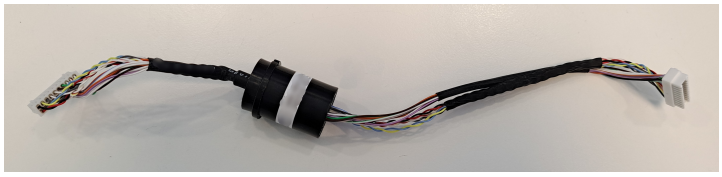

(a)

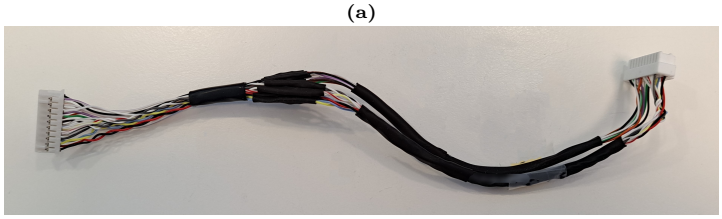

(b)

Figure 3.9: The slip ring and the cables with the slip ring part removed, figure A is the slip ring and figure B is the cables without slip ring.

3.9 The metal sandwich

When comparing the measurements in figure 4.6 of the PCBs spread out on the board to the measurements of the whole camera the curves look completely different, because of all the conductive material added around the PCBs and other

connected parts, these devices under test are completely different systems. The interesting part is that these systems have the same electrical source the emissions originate from.

To investigate how the 125MHz signal gets affected by the surrounding metallic parts the test "metal sandwich" was created. Where multiple measurements are done and for each measurement, a new part of the metal construction is added to the PCBs. Firstly a standard measurement was conducted with the PCBs on their holders on the board, then a compact version was measured where the PCBs were placed in a manner representing their placement inside the actual camera, just like the previous sandwich test. Then the metal parts, camera tilt unit, pan unit, and cassis were added one by one to the DUT, as visualized in figure 3.10. The result of the measurements is summarised in figure 4.20. To make all measurements in a uniform way the GND cable was not used inside the chamber, only the STP cable was connected to the DUT for all stages.

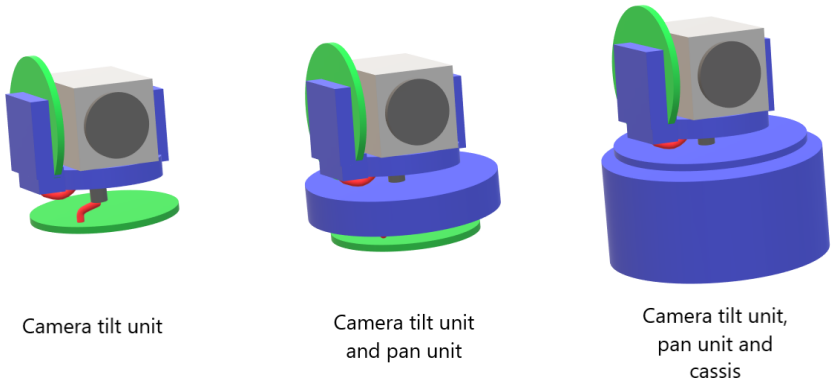

Figure 3.10: Illustration of the added metal parts, camera tilt unit, pan unit, and cassis in the metal sandwich test. The blue parts represent the added metal.

Result

In this chapter, the results of the tests described in chapter 3 Method are presented following the same structure as in the Method. The program used for measuring is limited in the comparing of data sets so the raw data was exported and analyzed using custom graphs in Matlab, an example of the code is in appendix A.

4.1 Initial tests

The results from the initial testing with the chamber setup and sniffing with near field probes. The first spectrum scan of the PCB can be viewed in figure 3.5 in chapter 3, and the results from sniffing with near field probes are found below.

4.1.1 Sniffing with near field probes

Sniffing with the near field probes on the PCBs, the 125MHz signal and its harmonics were found. Then, through cross-referencing with component specifications and analyzing the PCB layout, the source was identified to be a clock signal between two components on the PCB. With the signal path going from one component at the top layer to the other on the bottom layer through a via as illustrated in figure 4.1.

Figure 4.1: Illustration of how the interfering signal is routed on the PCB board, where the lighter, yellow line is the signal and the darker, orange represents the GND plane.

4.2 Resonance and Emission from connecting wires

In this section, the results from the resonance and emission measurements for the connecting wires are presented. The resonances found in the cables with the network analyzer are declared in table 4.1. Figure 4.2 displays the results of the first comparative measurements done with two ferrites on the wires connecting the different PCBs and camera block, where the measurements were done in table position 0° with horizontal antenna polarisation. The results for the measurements done through the auto test with all eight table positions and both antenna polarizations are presented in figures 4.3, 4.4, and 4.5, and in table 4.2 the peaks of the 125MHz harmonics are summarized.

Connection	Frequencies in MHz
Main - slip ring	109, 179, 210
Main - camera block, both wires	106, 205
Main - camera block, green wire	70-175 (max in 167), 206
Main - camera block, black wire	50-110 (max in 101)

Table 4.1: Measured resonance in the wires between the main PCB and slip ring and main PCB and camera block.

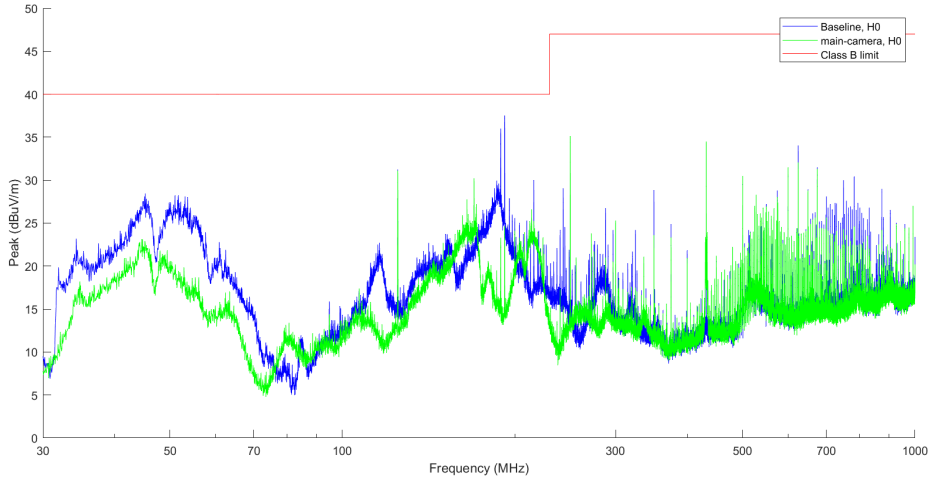

(a) Ferrites on the connection between the main board and camera block. The dark blue is the baseline without ferrites and the lighter green is with ferrites

Figure 4.2: Comparative A/B tests on the impact of two 742 711 32 ferrites on the different connections between power board, slip ring, main board, and camera block. Measured with the table in position 0°from the start position and horizontal polarisation on the antenna. The figures include the limit line for Class B compliance requirements, which is the line at the top.

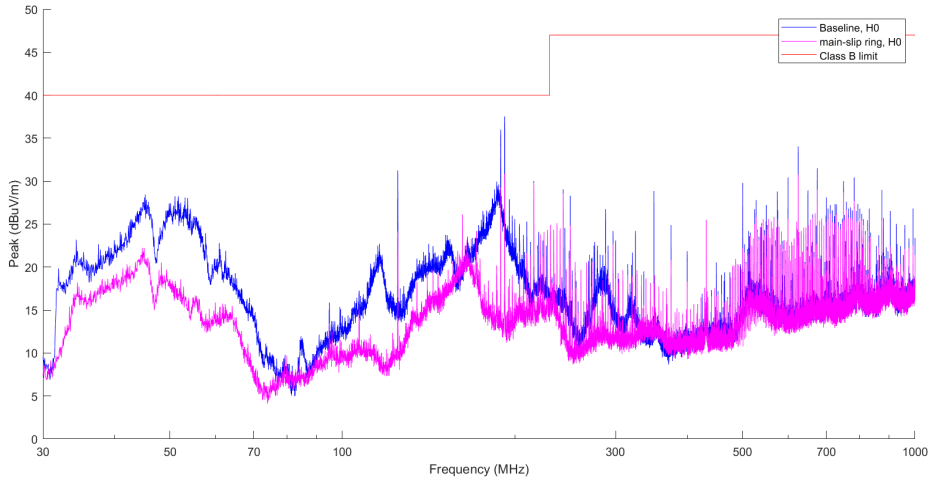

(b) Ferrites on the connection between the main board and slip ring, the dark blue is the baseline without ferrites and the lighter pink is with ferrites

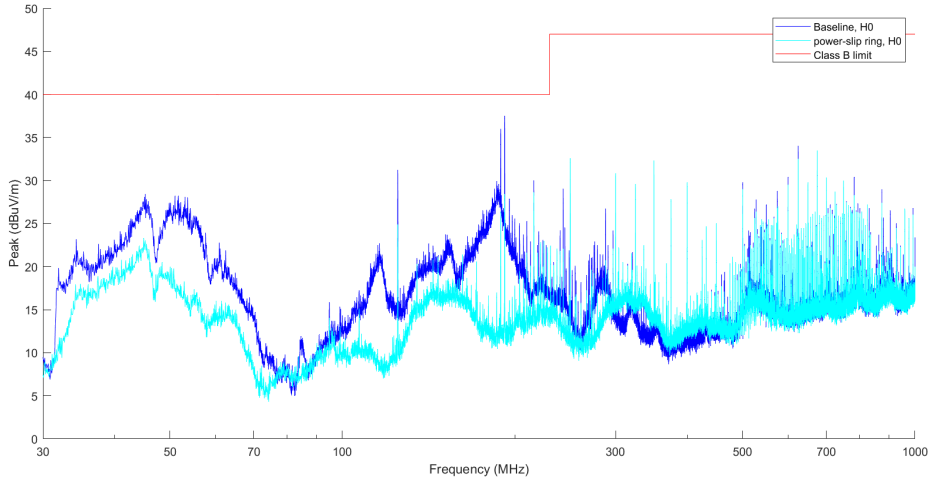

(c) Ferrites on the connection between the power board and slip ring. The dark blue is the baseline without ferrites and the lighter blue is with ferrites

Figure 4.2: Comparative A/B tests on the impact of two 742 711 32 ferrites on the different connections between power board, slip ring, main board, and camera block. Measured with the table in position 0°from the start position. The figures include the limit line for Class B compliance requirements.

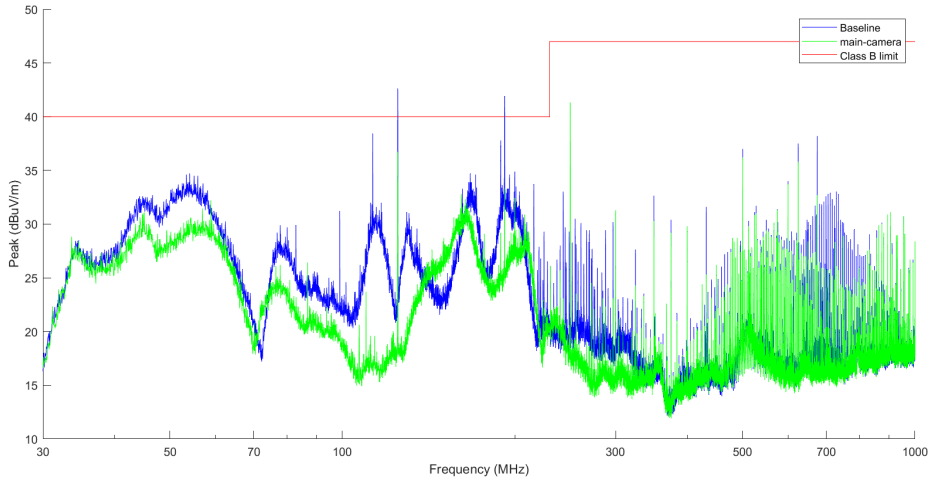

Figure 4.3: Comparative tests of two 742 711 32 ferrites on the wires between the main board and camera block against the baseline measurement with no ferrites. The measurements are done through Auto-test, registering the highest values from eight directions for both horizontal and vertical antenna polarisation. The darker blue curve is the baseline and the lighter green is with the ferrites, the top line is the limit line for Class B compliance requirements.

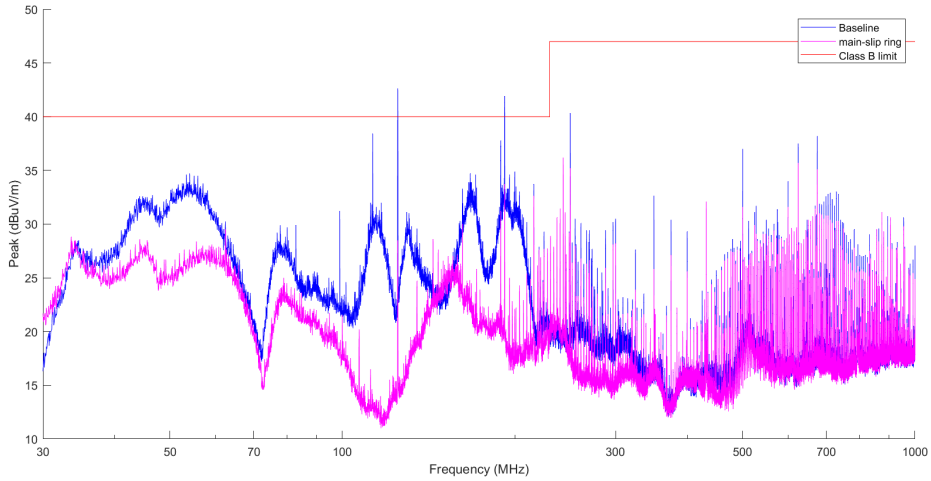

Figure 4.4: Comparative tests of two 742 711 32 ferrites on the wires between the main board and slip ring against the baseline measurement with no ferrites. The measurements are done through Auto-test, registering the highest values from eight directions for both horizontal and vertical antenna polarisation. The upper blue curve is the baseline and the lower pink is with the ferrites, the top line is the limit line for Class B compliance requirements.

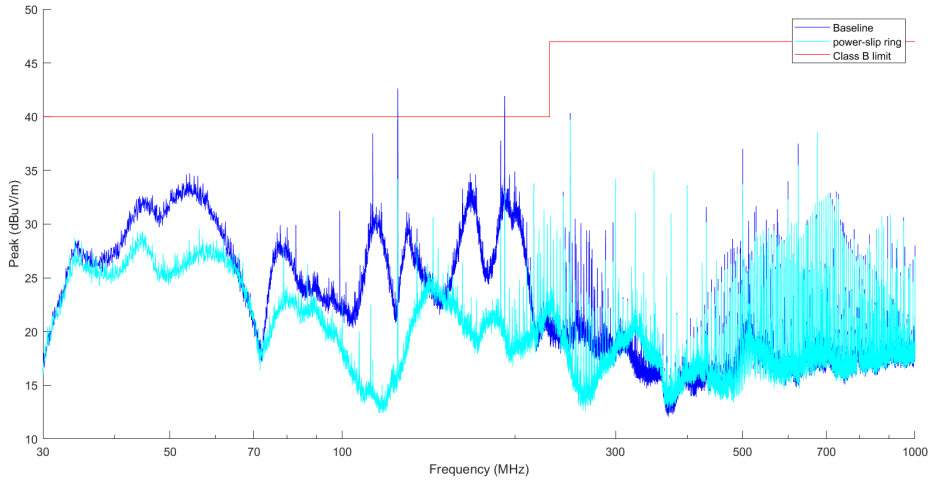

Figure 4.5: Comparative tests of two 742 711 32 ferrites on the wires between the power board and slip ring against the baseline measurement with no ferrites. The measurements are done through Auto-test, registering the highest values from eight directions for both horizontal and vertical antenna polarisation. The dark blue curve is the baseline and the light blue is with the ferrites, the top line is the limit line for Class B compliance requirements.

Freq MHz	Peak, $dB\mu V/m$				Difference, $dB\mu V/m$		
	Base-line	Test C Main-Camera	Test B Main-Slip ring	Test A Power-Slip ring	Main-Camera	Main-Slip ring	Power-Slip ring
125	42.6	36.7	28.5	34.2	-5.9	-14.1	-8.4
250	40.3	41.3	35.2	39.7	1	-5.1	-0.6
375	30.4	29.2	27.1	31	-1.2	-3.3	0.6
500	37	36.2	31.6	33.7	-0.8	-5.4	-3.3
625	37.5	35.8	35.7	35.5	-1.7	-1.8	-2
750	30.1	28.9	29.6	28.9	-1.2	-0.5	-1.2
875	30.1	30	31.1	30.7	-0.1	1	0.6

Table 4.2: The 125MHz harmonics peaks with ferrites on the connections. Baseline without any ferrites and then two 742 711 32 ferrites on the wires between the main board and camera block, main board and slip ring, or power board and slip ring. Test A, B and C refer to the visualised ferrite placement in figure 3.6. The difference in amplitude relative to the baseline is on the right in the table.

4.3 Whole camera vs PCBs

In this section, the results of the measurements comparing the whole camera vs PCBs as described in 3.7.2 are presented.

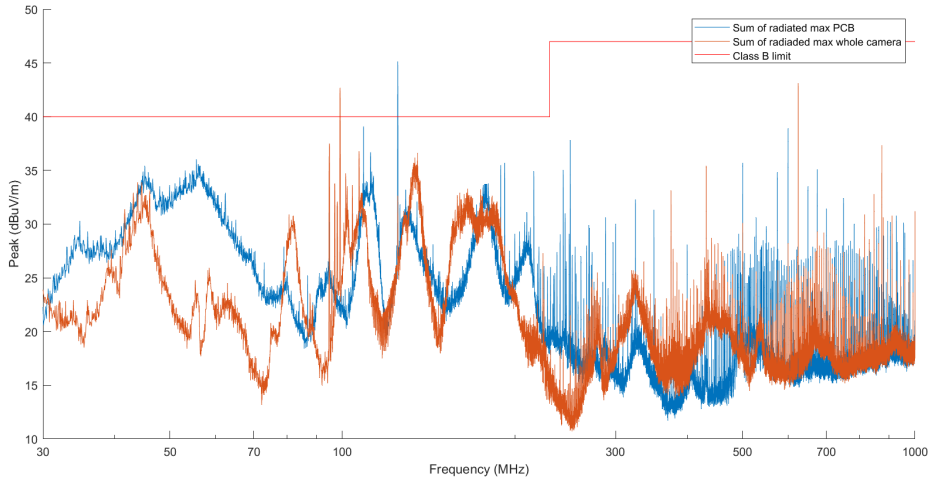

Figure 4.6: Comparing the emission from a whole camera against the PCB setup. The camera measured is camera 1 and measurements are made from all eight directions with both vertical and horizontal polarisation on the antenna, the cable setup for the camera was as illustrated in figure 3.4b with separated ethernet and ground cable. The blue top curve is the PCBs and the orange bottom curve is the whole camera, the straight line at the top is the limit line for Class B compliance requirements.

4.4 Sandwich test

This section presents the results from the "sandwich test" which compares the whole camera and the spread-out PCBs against the compactly placed PCBs.

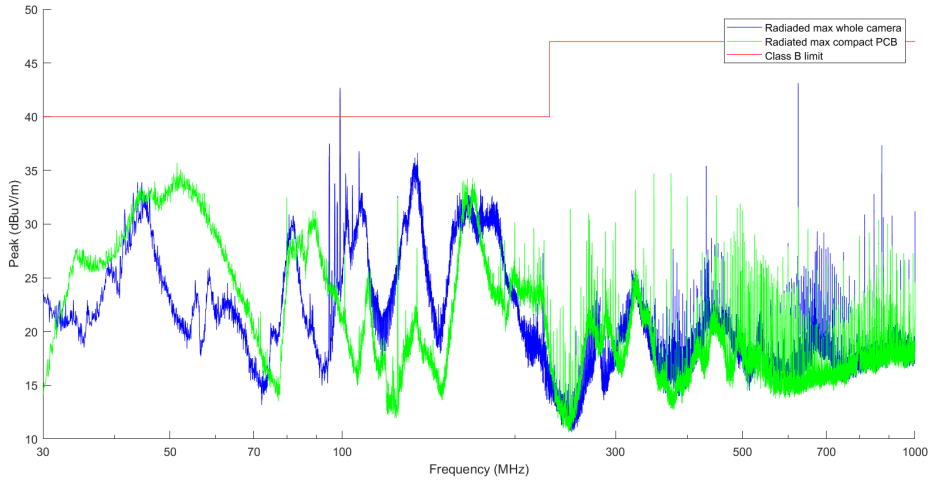

Figure 4.7: Comparing Measurements of a whole camera against the compact PCBs where the PCBs are placed in a compact way representing their placement in the camera. The darker blue curve is the whole camera and the lighter green is the compact PCB, with the limit line for Class B compliance requirements being the straight line at the top.

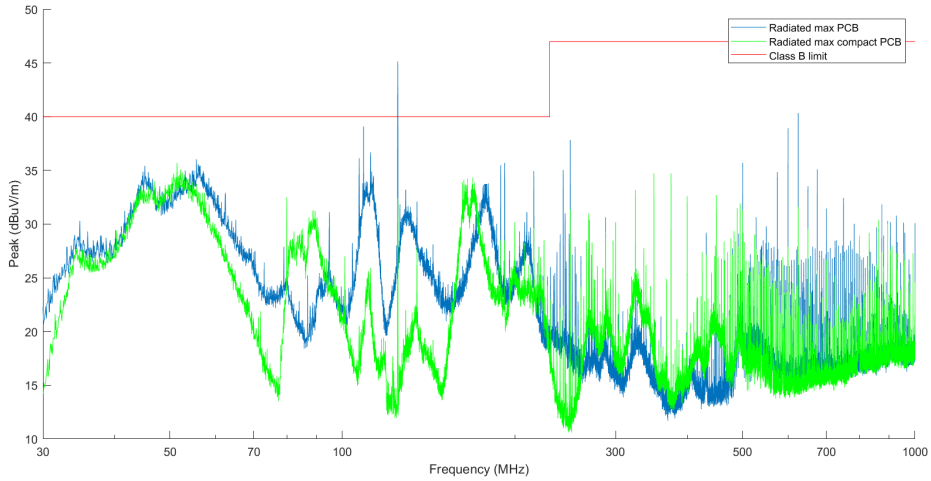

Figure 4.8: Comparative measurement of the PCBs placement, with the PCBs spread out vs placed in a compact way representing their placement in the camera. The darker blue curve is the spread-out PCBs and the lighter green is the compact PCB, with the limit line for Class B compliance requirements being the straight line at the top.

4.5 Comparing whole cameras

In this section are the results of the tests comparing whole cameras. Figure 4.9 is the first comparison of three different cameras, and in figure 4.10 is the before and after the ground contact spring was pressed on camera 2 as described in 3.7.4. These measurements were later redone in a better more improved manner with the results presented in figures 4.11, 4.12 and 4.13 as well as in section 4.8.

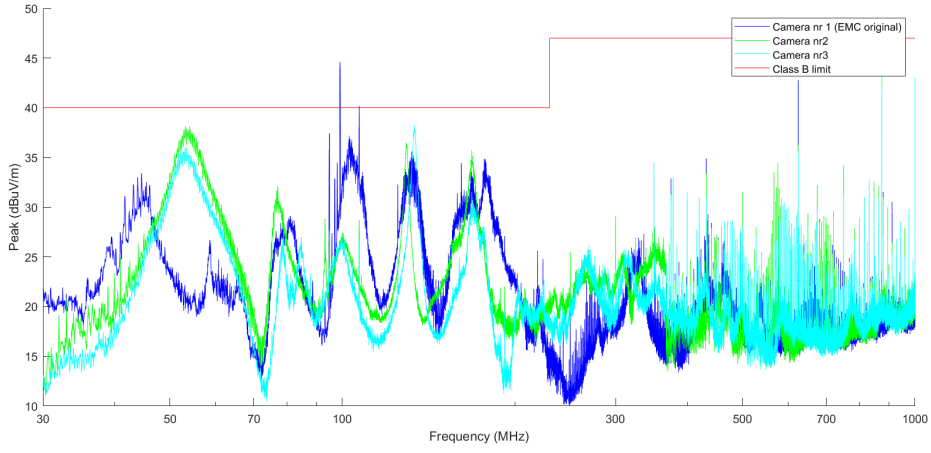

Figure 4.9: Measurements of three cameras made on two different occasions with possible differences in setup. A known difference between cameras is that camera 1 has the IR LEDs enabled and cameras 2 and 3 have the IR LEDs disabled, camera 1 is also an older camera model. The straight line at the top is the limit line for Class B compliance requirements.

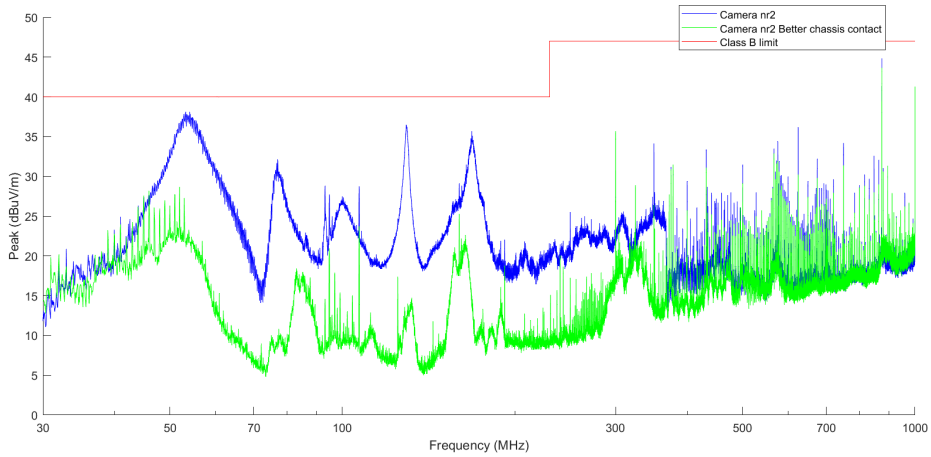

Figure 4.10: Comparing before and after the contact spring was pressed to create better contact between the power board GND and chassis GND on camera 2, the upper blue curve is before and the lower green curve is after the spring was pressed. Measurements were done through auto-test. The straight line at the top is the limit line for Class B compliance requirements.

Improved setup

The results from the improved testing of the whole camera are presented below. The comparison between cameras 1 and 3 is shown in figure 4.11, and in figure 4.12 and 4.13 is the before and after the contact spring was pressed for camera 3 and 4. Figure 4.14 is the result of camera 1 measured on two different occasions.

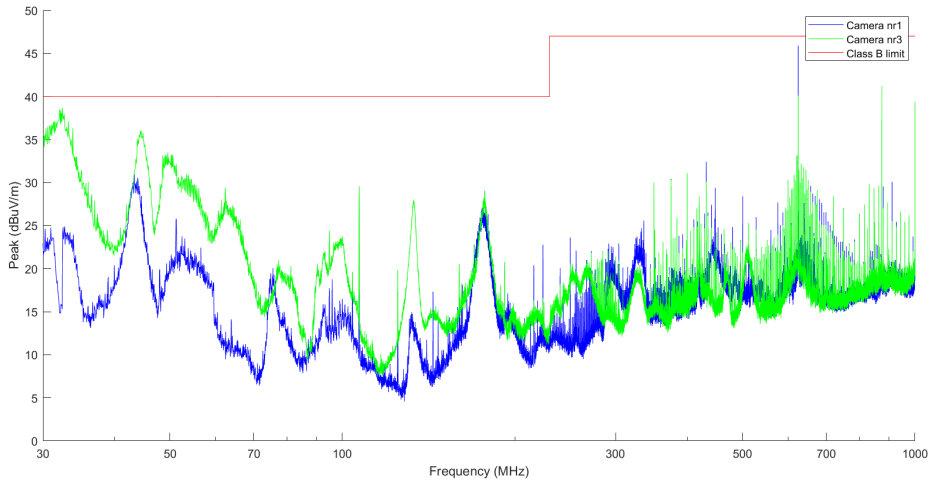

Figure 4.11: Comparative test between cameras 1 and 3 with the ethernet and GND cables twisted and taped together and pulled straight down to the floor through the table as depicted in figure 3.4c. Camera 1 is an older camera model. The upper green curve is camera 1 and the lower blue curve is camera 3, the straight line at the top is the limit line for Class B compliance requirements.

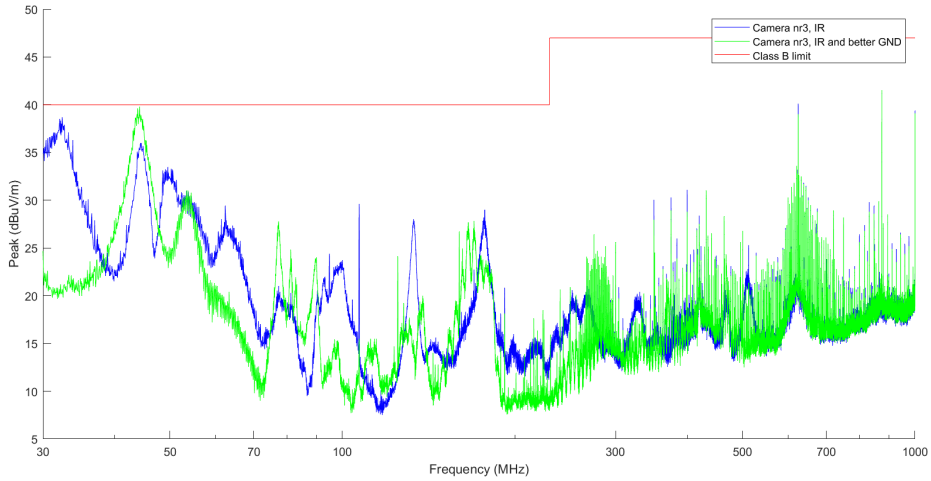

Figure 4.12: Comparing camera 3 before and after the contact spring was pressed for better contact. Measurements were done through auto test and with ethernet and GND cables twisted and taped together going straight down through the table to the floor as visualized in figure 3.4c. The darker blue curve is before the contact spring was pressed and the lighter green curve is after, the straight line at the top is the limit line for Class B compliance requirements.

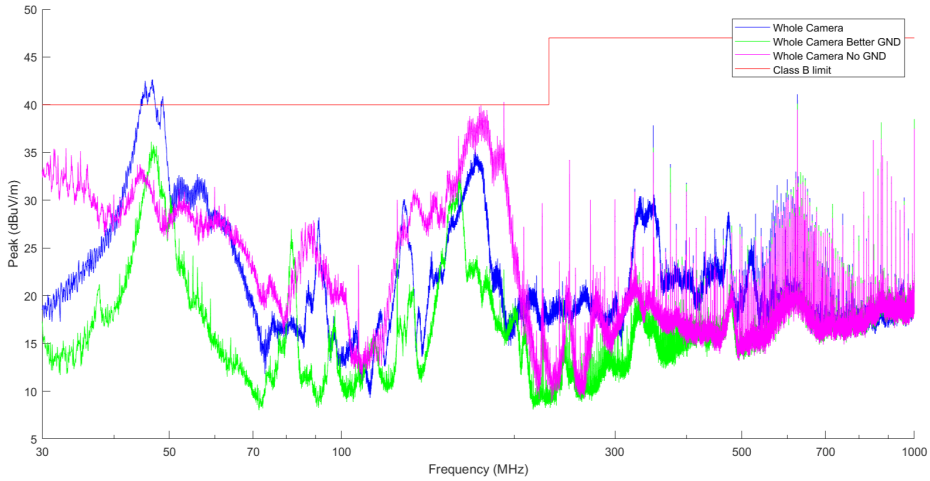

Figure 4.13: Comparing camera 4 before and after the contact spring was pressed for better contact as well as with the contact spring removed. Measurements were done through auto test and with ethernet and GND cables twisted and taped together going straight down through the table to the floor as shown in figure 3.4c. The darker blue curve (starting in the middle) is before the contact spring was pressed and the lighter green curve (starting at the bottom) is after. The pink curve (starting at the top) is with the contact spring removed and the straight line at the top is the limit line for Class B compliance requirements.

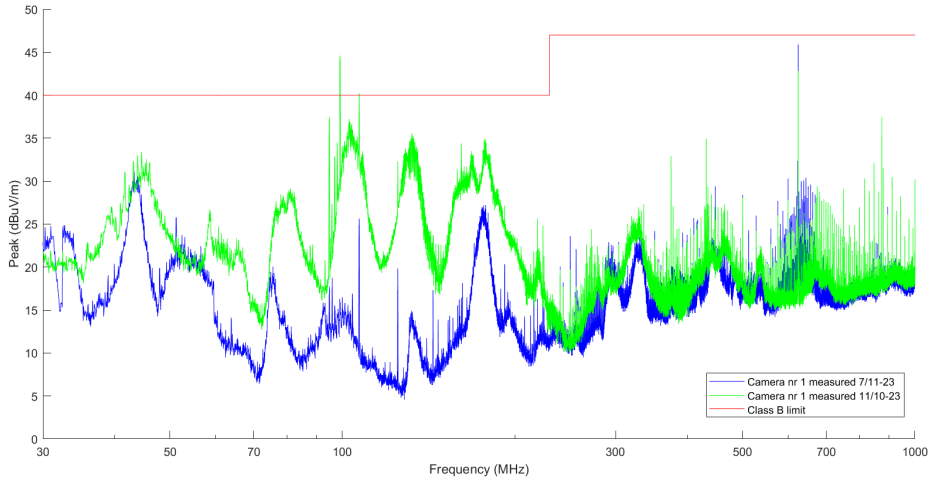

Figure 4.14: Camera 1 measured on two different occasions and with some differences in cable setup, with the measurement done the 11/10 having ethernet and GND cable separated as shown in figure 3.4b, while the 7/11 measurement having them close together as shown in figure 3.4c. The lighter green curve was measured the 11/10 and the darker blue curve the 7/11. The straight line at the top is the limit line for Class B compliance requirements.

4.6 Investigating the setup

In figures 4.15, 4.16, and 4.17 are the results of the chamber measurements, showing the level of RF radiation leaking into the chamber dependent on the cables used outside of the chamber and what port they are connected to.

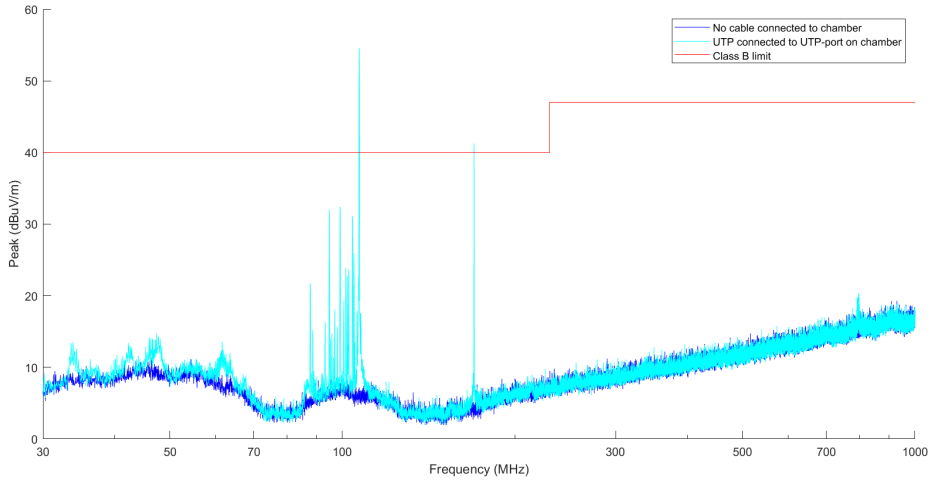

Figure 4.15: Measurements of the radiation inside the chamber with a non-powered camera connected inside of the chamber with loose UTP cable connected to the chamber's UTP-port. The dark blue curve at the bottom is the chamber baseline without any cables connected to it, and the lighter blue on top is with the UTP cable connected. The straight line at the top is the limit line for Class B compliance requirements.

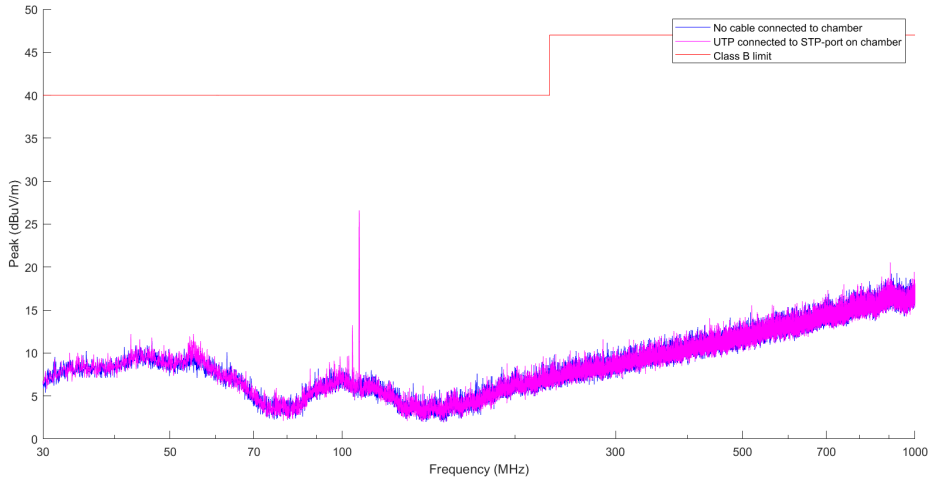

Figure 4.16: Measurements of the radiation inside the chamber with a non-powered camera connected inside of the chamber and loose UTP cable connected to the chambers STP-port. The dark blue curve at the bottom is the chamber baseline without any cables connected to it, and the pink on top is with the UTP cable connected. The straight line at the top is the limit line for Class B compliance requirements.

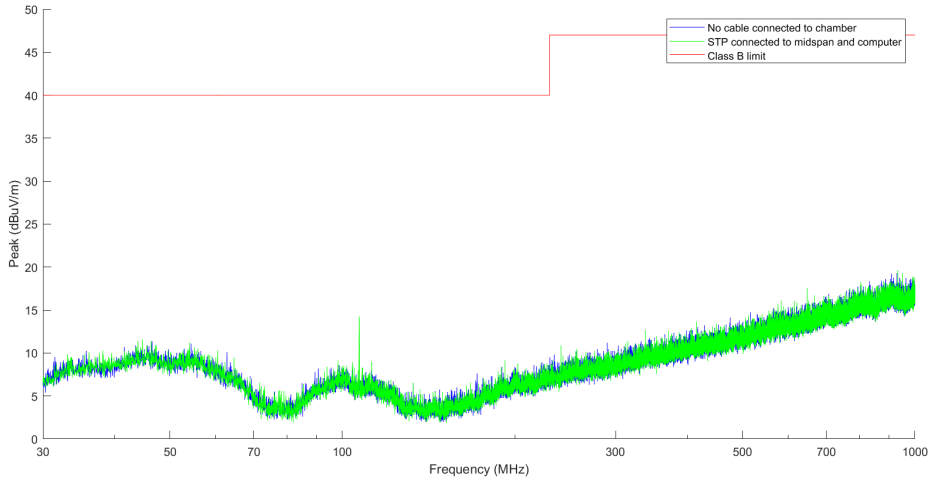

Figure 4.17: Measurements of the radiation inside the chamber with a non-powered camera connected inside of the chamber, an STP cable connected to the chamber's STP-port, and a non-powered midspan connected to the computer outside the chamber. The dark blue curve at the bottom is the chamber baseline without any cables connected to it, and the lighter green on top is with the STP cable connected. The straight line at the top is the limit line for Class B compliance requirements.

4.7 Slip ring testing

The results of the slip ring comparisons are shown in figure 4.18 and 4.19.

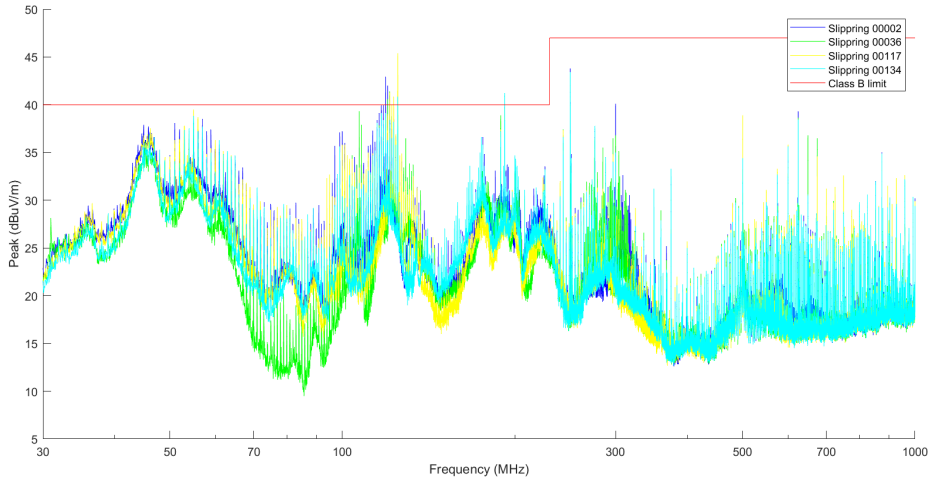

Figure 4.18: The results of the measurements comparing four different slip rings. Measurements are done through auto test recording the highest emissions from all eight directions for horizontal and vertical antenna polarisation. The Class B limit line is added at the top of the figure.

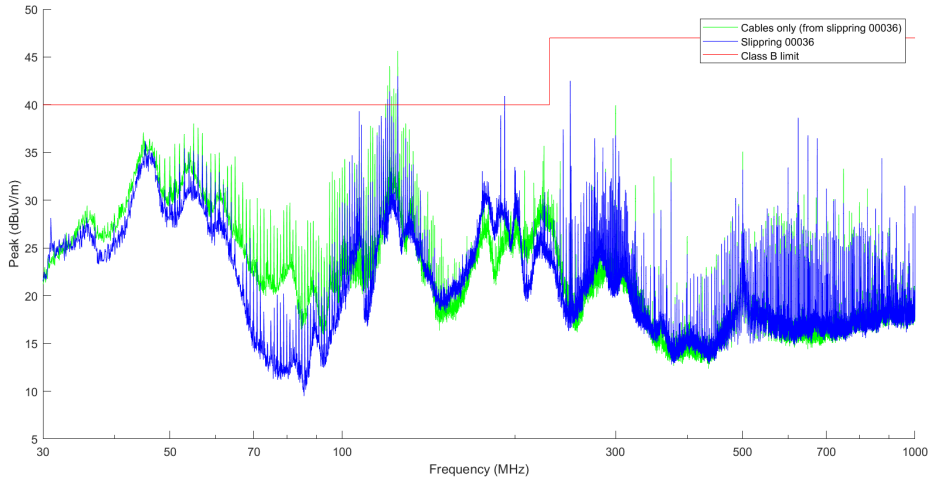

Figure 4.19: Results from the comparative measurements of the normal PCB setup against the setup with the slip ring removed and the cables directly soldered together. The darker blue curve is with the slip ring and the lighter green is without the slip ring. The Class B limit line is added at the top of the figure.

4.8 The metal sandwich

In this section are the results from the "metal sandwich" tests where the impact of the metal in the camera was tested. The measurements for the spread-out PCBs, the compact PCBs, and the whole camera are also compared with each other in figures 4.21, 4.22, and 4.23.

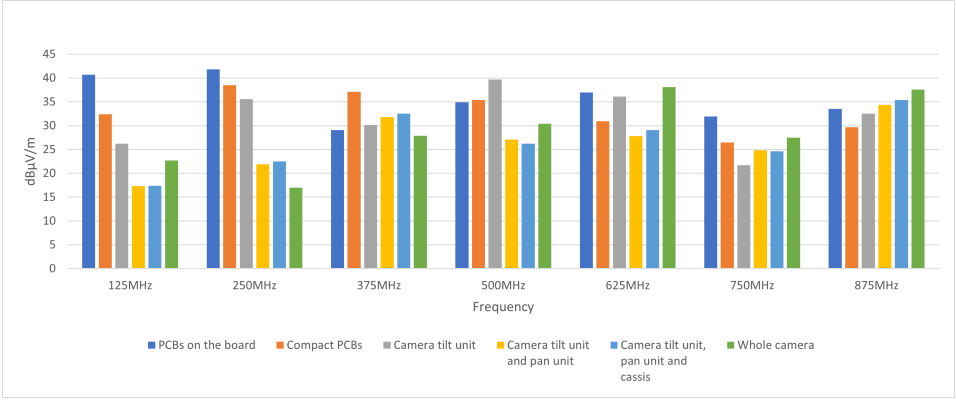

Figure 4.20: The results for the 125MHz signal and its harmonics when going from the bare, spread-out PCBs to the compact placement and successively adding the metal parts of the camera.

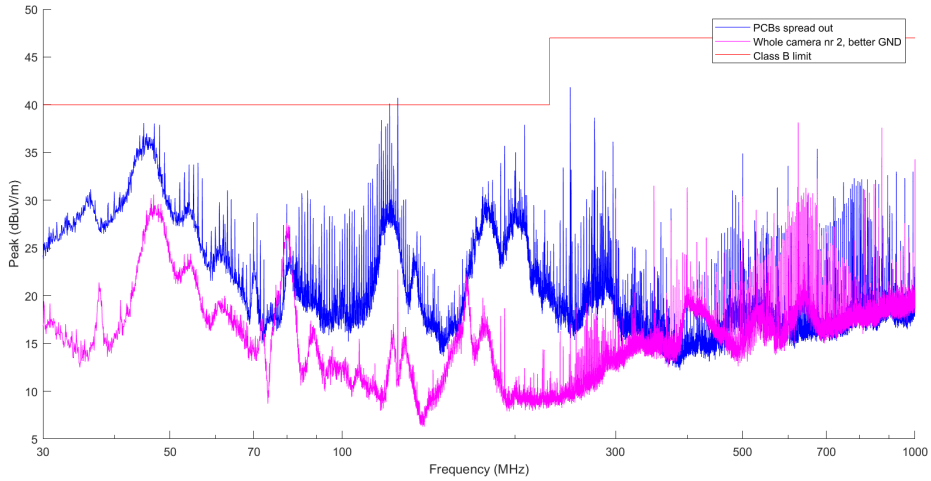

Figure 4.21: Comparing the PCBs when on the board setup against the whole camera. The camera measured was number 2 with the improved GND chassis contact. No GND cable connected. The upper blue curve is the PCBs and the lower pink is the whole camera. The Class B limit line is added in the figure.

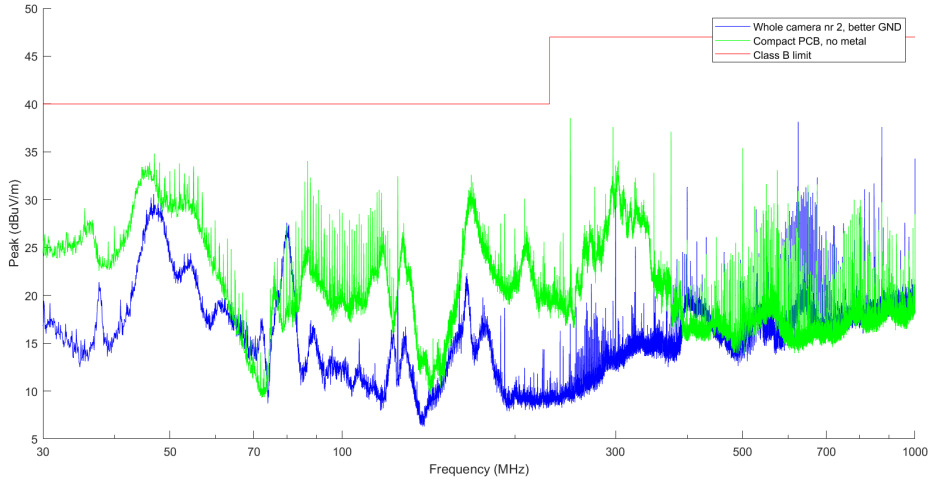

Figure 4.22: Measurements of camera number 2 with improved chassis GND versus the compact PCBs, where the PCBs are placed in a more compact manner representing their placement in the camera. The upper green curve is the compact PCBs and the lower blue is the whole camera. The Class B limit line is added in the figure.

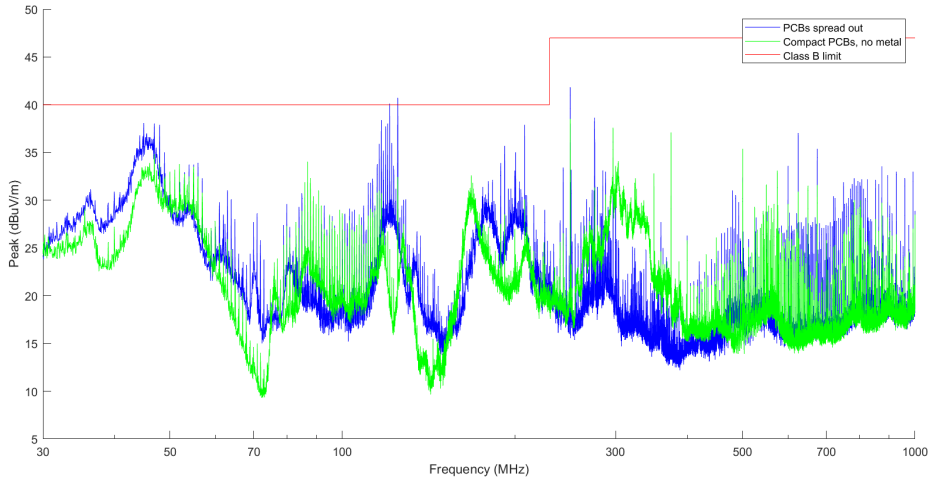

Figure 4.23: Comparing measurements of the spread-out PCBs and the compact placement of the PBCs. The darker blue curve is the PCBs spread out and the lighter green is the compact PCBs. The Class B limit line is the line at the top of the figure.

4.9 Result summary

Summarizing the results, figures 4.2 to 4.5 show the impact of ferrites on the different cables. The biggest effect on the clock signal for frequency 125MHz with the ferrites on the slip ring cable close to the main PCB.

The measurement comparing the whole camera and the bare PCBs in figure 4.6 visualizes the difference in emissions between the bare electronics of the camera compared to the whole finished product. This is further shown in section 4.4 with comparisons with a compact positioning of the bare PCBs, and in 4.8 with the gradual adding of the metal structure of the camera.

The results in section 4.5 show the impact of the ground connection to the camera chassis and the difference that can occur for the same DUT measured on different occasions.

Investigating the setup, section 4.6 presents the impact the choice of cables used outside the chamber has on the leakage into the chamber.

The results from testing the slip ring in section 4.7 show no difference between the different slip rings used and little to no difference for cables without the slip ring mechanics.

Discussion

In this chapter, the project and results will be discussed. Firstly the process of the project will be analysed and the testing approach evaluated. Then the measurement results will be analysed and possible conclusions drawn. Lastly, suggestions and discussion of possible improvements and further testing and research will be brought forward.

5.1 Evaluating the testing approach

Because an evaluation-based testing approach was used, where new tests were formed from evaluating the previous results, both the tests executed and the manner of execution were highly flexible and could be tweaked and improved along the progression of the project. This allowed for more suitable testing to be formed when problems arose, without changing the testing approach. Due to the nature of EMC problems, all of the necessary tests cannot be deduced beforehand. Therefore, by having a dynamic test plan, more specified testing can be achieved, yielding more accurate results. However, this requires time and plenty of knowledge in the applied field, which in this project is EMC.

5.2 Investigating the setup

Looking at the result in section 4.6 'Investigating the setup', high levels of FM band frequencies can be seen in some of the scenarios. For the Loose UTP cable connected to the chamber's UTP port high levels of the FM band are leaking into the chamber as seen in figure 4.15. However, just changing the chamber port used and therefore cable inside the chamber to STP a lot of these spikes get significantly lower or even disappear as seen in 4.16. Leakage into the chamber can be further reduced by the use of an STP cable on the outside connected to a non-powered midspan with the result in figure 4.17. This is a prime example of when the zoning is not correctly implemented. When connecting a UTP cable to the UTP port of the chamber the two different zones become connected and the outside noise is brought into the chamber, removing the shielding benefits of the chamber. When connecting the UTP cable to the STP port we shield the radiating cable inside the chamber and the noise reaching the antenna is decreased. Taking it a step further and using an STP cable outside the chamber, the shielding of the chamber is extended to include the cable on the outside, and the emissions outside the chamber are no longer picked up by the cable, thus lowering the noise inside the

chamber further. To strengthen the barrier between the two zones, common mode filters can be used as well. From the results in figure 4.15, 4.16, and 4.17 the conclusion can be made that there are no filters on the input ports of the chamber to filter out the unwanted frequencies absorbed by the cable outside the chamber.

5.3 125MHz signal

Investigating with a near field probe and viewing the signal path of the 125MHz signal as illustrated in figure 4.1 reveals that the signal return plane is not properly implemented which can create problems with common-mode radiated emissions. As described in section 2.1.5 when layer jumping with high-bandwidth signals it is important to couple the return path via tightly to the signal path to maximize the magnetic flux cancellation. If the RF return current does not closely follow the trace of the signal, undesired common-mode currents will likely develop, resulting in common-mode radiated emissions.[3, pp. 98–99] The return path for the 125MHz signal is not closely coupled to the signal the entire way. There are ground planes close to the horizontal signal trace. However, when switching layers through the via, there are no connections between the two ground planes nearby for the return current. Because of this, there is no telling what path has the lowest inductance for the return current to take. Deducing what impact this has on the radiated emissions from the camera would need a greater extent of work and testing.

From table 4.2 the biggest impact the ferrites have is on the frequency 125MHz when placed between the main board and slip ring and the second biggest is between the power board and slip ring for the same frequency. This shows that this is a path used by the interfering signal and that it originates from the main board since the emissions are affected more when the ferrites are placed close to the main board. This is further corroborated when looking at the cable resonances in table 4.1, it can be expected that the biggest effect on the amplitude is at the frequencies around 100MHz to 200MHz since this is where the resonant frequencies are found in the cables and therefore the impedance in the cable is lower around these frequencies. When adding the ferrites to the cable we add about 200-300 Ω of impedance per ferrite which results in a larger impact on the amplitude for currents with frequencies that had previously low impedance in the wire, compared to the currents with frequencies that already have a relatively higher impedance in the cable.

There is a dip for the 125MHz signal when the ferrites are placed on the cables between the main board and the camera block as well. It is not a significant dip but it can indicate that the cable connection is somehow a part of the system creating the interference. Because everything is connected, either directly through wires and components or parasitically through proximity, all changes can affect the measurements. Even if the changes are not made in a significant part of the structure, the change alters the characteristics of the structure/environment that can impact how the emissions behave. Because of this and the measurement uncertainty, we can only trust the findings when seeing a significant change in outcome from the adjustments made on the DUT. For this chamber setup, the rule of thumb is $6dB\mu V$ for deciding if a change in amplitude is of interest.

Since there is a lot of difference between the bare PCBs spread out on a board compared to the entire camera with motors and metal chassis etcetera, the signals seen as strong when measuring the PCBs might not be the same signals that are

coming through and showing high amplitude for the whole camera. The change in amplitude for the 125MHz harmonics when systematically adding more and more of the metallic camera parts is presented in figure 4.20. Here the emissions of the first harmonic on 125MHz decrease with the added metal parts while the higher harmonics of 625MHz and 875MHz increase in amplitude. All the signals are coming from the PCBs even if they are not seen as significant when measuring on the PCB. In this example, we can see how the 125MHz signal might look like a problem when measuring the PCBs alone, but ends up not being problematic for the finished product, instead higher frequencies of its harmonics are increased which could create problems instead.

This will look very different between different products but knowing that the emissions come from the same signal on the PCB and then rectifying the reason it can propagate out can fix multiple and different emission problems for different products.

5.4 Chassis ground connection

Analyzing the results from the tests done on the chassis ground connection in figures 4.10, 4.12 and 4.13 there is a big variation between the different cameras and the effect pressing the GND connection has on the emissions from them. Because of this significant variation, no conclusions can be drawn about the ground connection and its quality. All we can see is that pressing the spring connecting the chassis ground has some effect on the emissions for all cameras, however why this is cannot be said. There is a large human factor in this experiment since the ground spring has been pressed by hand and can have been done differently for the different cameras, with for example different forces and angles.

5.5 Slip ring testing

Comparing the emissions from the PCB boards with and without the slip ring in figure 4.19 and the different slip rings in figure 4.18 we can see how little difference the rotating part is making for the RF emissions. The only deviation between the curves in figure 4.19 are between 65MHz to 100MHz and when investigating the various slip rings in figure 4.18, one cable deviated from the rest. This same cable gave more similar results to the other slip rings measured when it was converted into a slip-ring-free cable.

5.6 Project aims

The project aimed to create a test setup for a specific camera product and a testing method for investigating EMC problems that could be used for multiple projects and products, as well as using this to investigate a common interference problem in the specified camera. The aim was divided into the three following goals.

- Construct a test setup for the chosen camera and the camera components that are of interest.
- Bring forth a testing plan and method to identify interfering sources and investigate them.

- Use this plan and method to identify a common interfering source and investigate it.

All three of these goals were realized during the project, the first and second goals were straightforward, to create a test setup to perform uniform testing and specify a testing method. The test setup was realized by modeling and 3D printing stands for the camera parts and mounting them on a wooden slab, and the method to be used was decided to be A/B tests formed by analyzing previous results. The test method process was developed and explained/visualized in a flowchart in figure 3.1, and can be used for testing of other products. However, the test setup cannot be used as is for other products but may serve as inspiration.

The final goal was to use the setup and method to investigate the specified camera. This was the most time-consuming and difficult part of the project because of the method used there is no exact formula or pre-set tests to use, so the work done needed to be continuously analyzed throughout the working process.

5.7 Future research

Because of the limitations of this project the theory that the routing of the clock signal on 125MHz is the reason why the signal and its harmonics radiate from the DUT could not be confirmed or denied. To investigate this further, changes to the PCB routing need to be done and tested. A possible way to test the theory is to make minimal changes to the PCB routing in the form of adding vias close to the signal via for the return current to go through. Then a new PCB with this change needs to be printed and A/B tests can be performed on the different PCBs.

Further research could also be done on the chassis ground connection. The results from the testing, although varying for each camera, showed that improving the connection between the chassis and power PCB affected the emissions from the camera. However, the results are not reliable because of the considerable human factor, and further improved research and testing could be of interest.

This thesis has focused on one common interfering challenge when developing camera products, and the work done on this can be applied, replicated and modified for additional EMC challenges. Using the same method to identify and find solutions to common interferences facilitates the development process and reduces the need for EMI troubleshooting.

Conclusions

Through analyzing the results of the thesis some interesting discoveries have been made. For some, conclusions can be drawn, while others require further testing and research.

The resulting conclusions made are the following,

- The source of a 125MHz radiated emission and its harmonics was identified to be the clock signal between two components on the PCB. While the routing of the signal is believed to be the root of the radiated emission it could not be verified and more complex testing is needed to confirm this to be the emission origin.
- The slip ring was demonstrated to not affect the emissions of the DUT in any significant way.
- The measurements testing the connection of the chassis GND spring gave varying results and no conclusions could therefore be drawn. However, it can be of interest to test this further through tests with less human impact.
- During the project the anechoic chamber used was investigated which gave the conclusion that the use of STP cables was needed outside of the chamber to keep the zoning in the chamber intact and not compromise the shielding.

Overall the testing approach used has been successful and has been a productive approach for the project and the project goal.

References

[1] M. Mardiguian, *Controlling Radiated Emissions by Design*. Chapman & Hall, New York, NY, 1992, ISBN: 0-442-00949-6.

[2] T. Williams and K. Armstrong, *EMC for Systems and Installations*. Newnes, 2000, ISBN: 0 7506 4167 3.

[3] M. I. Montrose, *EMC Made Simple, Printed Circuit Board and System Design*. Montrose Compliance Services, Inc, 2014.

[4] R. Dockey and R. German, "New techniques for reducing printed circuit board common-mode radiation," in *1993 International Symposium on Electromagnetic Compatibility*, 1993, pp. 334–339. DOI: 10.1109/ISEMC.1993.473716.

[5] C. Paul, "A comparison of the contributions of common-mode and differential-mode currents in radiated emissions," *IEEE Transactions on Electromagnetic Compatibility*, vol. 31, no. 2, pp. 189–193, 1989. DOI: 10.1109/15.18789.

[6] M. van Doorn, "Radiated emission from signal traces changing reference planes," in *2014 International Symposium on Electromagnetic Compatibility*, 2014, pp. 709–712. DOI: 10.1109/EMCEurope.2014.6930996.

[7] T. Williams, *EMC for Product Designers*. Elsevier, Newnes, 2017, ISBN: 978-0-08-101016-7.

[8] S. standards institute (SIS), "SS-EN 55032. Multimediautrustning - EMC-fordringar - Emission," in Stockholm:SIS, 2015.

[9] Keysight, *Network analysis*. [Online]. Available: https://www.keysight.com/us/en/solutions/measurement-fundamentals/network-analysis.html (visited on 12/29/2023).

[10] D. MacArthur, *What every electronics engineer needs to know about: Measuring receivers*. [Online]. Available: https://incompliancemag.com/what-every-electronics-engineer-needs-to-know-about-measuring-receivers/#:~:text=However%2C%20where%20oscilloscopes%20look%20at,signal%20on%20the%20horizontal%20scale. (visited on 03/06/2024).

[11] The American Radio Relay League, *The ARRL Antenna Book*. The American Radio Relay League, 1988, ISBN: 0-87259-206-5.

[12] P. J. Bevelacqua, *Antenna gain*. [Online]. Available: https://www.antenna-theory.com/basics/gain.php (visited on 12/30/2023).

[13] A. Bensky, *Short-range Wireless Communication*. Newnes, 2019, ISBN: 978-0-12-815405-2.

[14] P. Sanghera, "Chapter 6 - rfid+ selecting the rfid system design," in *RFID+ Study Guide and Practice Exams*, P. Sanghera, Ed., Rockland: Syngress, 2007, pp. 135–166, ISBN: 978-1-59749-134-1. DOI: https://doi.org/10.1016/B978-159749134-1.50010-4. [Online]. Available: https://www.sciencedirect.com/science/article/pii/B9781597491341500104.

[15] Electricity-Magnetism, *Dipole antennas*. [Online]. Available: https://www.electricity-magnetism.org/dipole-antennas/ (visited on 01/08/2024).

[16] Schwarzbeck Mess-Elektronik, 2007. [Online]. Available: https://commons.wikimedia.org/wiki/File:Schwarzbeck_UHALP_9108_A.jpg (visited on 11/13/2023).

[17] Rohde & Scharz, *R&S®HK116E biconical antenna*. [Online]. Available: https://www.rohde-schwarz.com/se/products/test-and-measurement/radiated-testing/rs-hk116e-biconical-antenna_63493-89408.html (visited on 01/15/2024).

Appendix

A Matlab code example

```
%Load the files into Matlab
C1 = readtable('Slippring 00002 23-11-08.xls');
C2 = readtable('Slippring 00036 23-11-08.xls');
C3 = readtable('Slippring 00117 23-11-08.xls');
C4 = readtable('Slippring 00134 23-11-08.xls');
C5 = readtable('Slippring 00036 Cables only (slipring part removed) 23-11-08.xls');


%Create limitline
y = [40 40 47 47];
x = [30 230 230.001 1000];
M5 = "Class B limit";

%Plot the curves in the same figure
figure(1);
hold on;
a1 = semilogx(C1{:,1},C1{:,2}, "-b");
M1 = "Slippring 00002";
a2 = semilogx(C2{:,1},C2{:,2}, "-g");
M2 = "Slippring 00036";
a3 = semilogx(C3{:,1},C3{:,2}, "-y");
M3 = "Slippring 00117";
a4 = semilogx(C4{:,1},C4{:,2}, "-c");
M4 = "Slippring 00134";

%Plot limit line and add legend, x- and y-label, ticks on x-axis
a5 = semilogx(x,y,"-r");
set(gca, 'XScale', 'log') %Set x-axis to log scale
legend([a1,a2,a3,a4,a5], [M1,M2,M3,M4,M5]);
xlabel('Frequency (MHz)');
ylabel('Peak (dBuV/m)');
xticks([30 50 70 100 300 500 700 1000]);

```

```
34
35 figure(2);
36 hold on;
37 a6 = semilogx(C5{:,1},C5{:,2}, "-g");
38 M6 = "Cables only (from slippring 00036)";
39 a2 = semilogx(C2{:,1},C2{:,2}, "-b");
40 M2 = "Slippring 00036";
41
42 a5 = semilogx(x,y,"-r");
43 set(gca, 'XScale', 'log')
44 legend([a6,a2,a5], [M6,M2,M5]);
45 xlabel('Frequency (MHz)');
46 ylabel('Peak (dBuV/m)');
47 xticks([30 50 70 100 300 500 700 1000]);
```

B Ferrite datasheet

Properties		Value	Unit	Tol.
Material		4 W 620		
Initial Permeability	μ_i	620		typ.
Curie Temperature	T_C	150	°C	typ.
Plastic Housing Color		Grey		
Plastic Housing Flammability Rating		UL94 V-0		
Test Cable		AWG26		
Test Cable Length		90	mm	
Cable Diameter		7 - 8.5	mm	

Typical Impedance Characteristics:

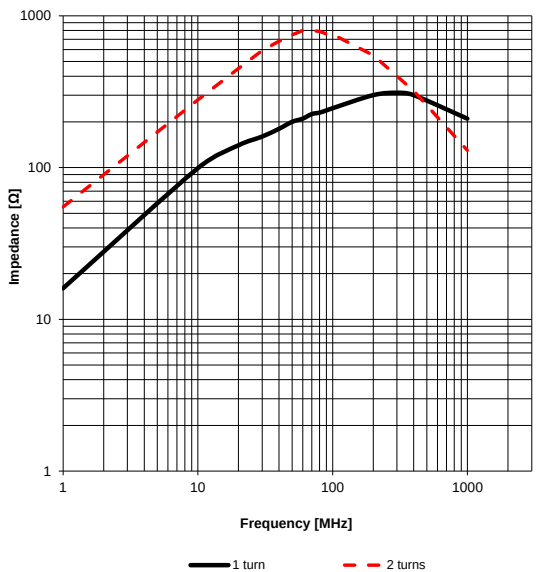

RoHS COMPLIANT · REACh COMPLIANT · HALOGEN FREE

WÜRTH ELEKTRONIK MORE THAN YOU EXPECT

Würth Elektronik eiSos GmbH & Co. KG
EMC & Inductive Solutions
Max-Eyth-Str. 1
74638 Waldenburg
Germany
Tel. +49 (0) 79 42 945 - 0
www.we-online.com
eiSos@we-online.com

CHECKED	REVISION	DATE (YYYY-MM-DD)	GENERAL TOLERANCE	PROJECTION METHOD
NFi	008.001	2021-05-10	DIN ISO 2768-1c	

DESCRIPTION: **WE-STAR-TEC Snap Ferrite with safety key technology**

ORDER CODE: **74271132**

BUSINESS UNIT	STATUS	PAGE
eiSos	Valid	2/6

Wurth Elektronik, *74271132 Datasheet WE-STAR-TEC Snap Ferrite with safety key technology* `https://www.we-online.com/components/products/datasheet/74271132.pdf`